Methods

Mice Genotyping

We genotyped offspring by PCR using the following primer sequences: Ctsk-Cre, P1N 5'-CCTAATTATTCCTTCCGCCAGGATG-3', P2N 5'-CCAGGTTATGGGCAGAGATTTGCTT-3', P3N 5'-CACCGGCATCAACGTTTTCTTTTCG-3', Plekhm1 floxed allele, LoxgtF 5'-TGAATCTGCTTGGTTGGTTG, LoxgtR 5'-CAAACTTCGGGGTTTGTTTG, Plekhm1 null allele, LoxgtF 5'-TGAATCTGCTTGGTTGGTTG-3', FrtgtR 5'-CTAAGCAGCCAAGGACAAGG-3'.

Antibodies and reagents

The antibodies and their applications are listed in Supplemental Table 6. The rabbit polyclonal antibody against the N-terminal portion of murine PLEKHM1 was generated and affinity purified by 21st Century Biochemicals (MA, USA). All chemical compounds were from Sigma-Aldrich. Cell culture alpha-MEM (78-5077EB) and 10 × Trypsin/EDTA (15400-054) were purchased from Life Technologies. High glucose DMEM (D-5648) and 10 × penicillin–streptomycin-l-glutamine (PSG) (G1146) were obtained from Sigma-Aldrich. Fetal bovine serum (FBS) was purchased from Hyclone.

Bone marrow monocyte (BMM) and osteoclast cultures

Whole bone marrow was extracted from tibia and femurs of one or two 8–10 week-old mice. Red blood cells were lysed in buffer (150 mM NH_4Cl, 10 mM $KNCO_3$, 0.1 mM EDTA, pH 7.4) for 5 minutes at room temperature. 5×10^6 bone marrow cells were plated onto a 100mm petri-dish and cultured in α-10 medium (α-MEM, 10% heat-inactivated FBS, 1 × PSG) containing 1/10 volume of CMG 14–12 (conditioned medium supernatant containing recombinant M-CSF at 1μg/ml) (1) for 4 to 5 days. Pre-osteoclasts and osteoclasts were generated by culturing BMMs (at density of 160/mm^2) with 1/100 vol of CMG 14–12 culture supernatant and 100 ng/ml of recombinant RANKL.

Osteoblast cultures

Primary osteoblasts were harvested from calvaria or cultured from bone marrow stromal cells as described in Supplemental Methods. Three to five calvariae/genotype were pooled and incubated with 4mM EDTA/PBS at 37°C for 10min for three times. The calvariae were then incubated through a serial digestion with 200U/ml collagenase (# 4196, Worthington)/PBS at 37°C for 15min with shaking. Cells in fractions 4-6 were collected and cultured at 5×10^5 cells/150mm culture dish in α-10 medium. Osteoblast differentiation (at 2.3×10^4 cells/well of 6-well plate) was induced by 1% Ascorbic Acid (A4544, Sigma-Aldrich) and 20mM β-glycerolphosphate (G6251, Sigma-Aldrich) α-10 medium. For osteoblast differentiation from bone marrow stromal cells, 5×10^6 whole bone marrow cells/well of 12-well plate were cultured with α-10 medium and 1% Ascorbic Acid/20mM β-glycerolphosphate for 14 or 21 days.

Mouse embryonic fibroblast (MEF) culture

E13.5 or E14.5 mouse embryos were washed with cold PBS and cleared out the head, limbs and internal organs. The rest of tissues were teased into small pieces and incubated with 5 × Trypsin/EDTA at 4°C overnight (2). The tissues were then incubated at 37°C for 30min. The digestion was stopped by D-10 medium (DMEM with 10% heat-inactivated FBS, 1 × PSG). The cells in the supernatant were centrifuged and were cultured with D-10 medium till confluent.

TRAP staining

BMMs were cultured on 48-well tissue culture plate in α-10 medium with M-CSF and RANKL for 4-5 days. The cells were fixed with 4% paraformaldehyde/phosphate buffered saline (PBS) and TRAP was stained with NaK Tartrate and Napthol AS-BI phosphoric acid (Sigma-Aldrich).

Alkaline phosphatase and bone nodule staining

Calvaria or bone marrow stromal cells were cultured with α-10 medium and 1% Ascorbic Acid/20mM β-glycerolphosphate for 14 or 21 days. Cells were fixed with 1:1 10% formaldehyde and ethanol for 10min and washed with PBS twice. Alkaline phosphatase was stained with a kit (86R-1, Sigma-Aldrich) according to the

manufacture's protocol. The mineralized bone matrix was stained with 2% Alizarin Red (pH 4.1-4.3) (A5533, Sigma-Aldrich) in osteoblasts fixed with 10% formaldehyde.

Resorption pit staining and medium CTx-I ELISA

Mature osteoclasts grown on bone slices were fixed with 4% paraformaldehyde/PBS for 20 minutes. After washing twice in PBS, the cells were removed from bone slices with a soft brush. The slices were then incubated with 20μg/ml peroxidase-conjugated WGA (Wheat germ agglutinin) lectin (L-7017, Sigma-Aldrich) for 30-60 min at room temperature. After washing in PBS twice, 0.52 mg/ml 3,3'-diaminobenzidine (D-5905, Sigma-Aldrich) was added onto the slices for 30 minutes. Samples were mounted with 80% glycerol/PBS. Medium CTx-1 concentration of day-5 OC culture was measured using CrossLaps for Culture ELISA kit (AC-07F1, ImmunoDiagnosticSystems) following the manufacture's instruction.

Lysosomal β-hexosaminidase exocytosis assay

Cells were trypsinized, counted and $4x10^4$ WT or KO cells were incubated or not with 300 ng/mL SLO (or without SLO, for controls) in 350 μl of cold PBS ($+Ca^{2+}$) on ice for 5 min, followed by incubation at 37 ^{0}C for 2 min. After 10 min centrifugation at 400 x the supernatants containing exocytosed lysosomal enzymes were incubated 1:1 with sodium citrate-phosphate buffer, pH 4.5, in the presence of 0.75 mM of -hexosaminidase substrate (4-methy-lumbelliferyl-*N*-acetyl-□-D-glucosaminide dihydrate (SIGMA - #M2133)) for 30 min. 100 μl of each sample were transferred to a 96 well plate and the reaction stopped with 25 μl of 2 M Na2CO3 and 1M glycine, pH 9.0. Readings were taken in ELISA plate reader (Spectra max – Molecular Devices) at 362 nm excitation / 448nm emission. To obtain total extracts cells were solubilized 1% NP40 in PBS. A dilution of the extracts (1:10) was used to determine the total β-hexoaminidase activity for each cell type and the exocytosis results were expressed as percentage of the total enzyme content in the cells.

***Coxiella burnetii* phagocytosis assay**

Bone marrow macrophages (BMMs) were cultured ($1x10^5$ cells per mL) on glass coverslips (microscopy) or in glass-bottomed tissue culture plates (mCherry expression) in RPMI 1640 medium with 10% fetal bovine serum

(FBS; Invitrogen) at 37°C and 5% CO_2. BMMs were infected with avirulent *Coxiella burnetii* (Nine Mile phase II, RSA 439) expressing mCherry (1) at an MOI of ~15 organisms, the same for microscopy and phagocytosis.

For microscopy, cells were washed 3 times with cold PBS then fixed and permeabilized with 100% cold methanol. After fixation, cells were washed 3 times with PBS and blocked in PBS containing 0.5% BSA overnight at 4°C. A monoclonal antibody against LAMP-1 (1:300, 1D4B, Developmental Studies Hybridoma Bank, University of Iowa, Iowa City, IA) was used to detect the *C. burnetii* parasitophorous vacuole. Rabbit anti-sera raised against *C. burnetii* was used to detect bacteria. 4′,6-diamidino-2-phenylindole (DAPI; Invitrogen) was used to detect host and bacterial DNAs. Coverslips were mounted in MOWIOL and visualized using a Nikon Ti-U microscope (Nikon). A D5-QilMc digital camera obtained images and analysis was performed using NIS-Elements software (Nikon).

For phagocytosis assays, fluorescence of mCherry-expressing *C. burnetii* was quantified in infected BMMs cultured in glass-bottomed plates using a SynergyHi Microplate Reader (585 excitation 620um emission, BioTek). Background from uninfected cells was subtracted from all samples to determine final mean fluorescence intensity (MFI).

RNA isolation and qPCR

Total RNA was purified using RNeasy mini kit (Qiagen) according to the manufacture's protocol. First-strand cDNAs were synthesized from 0.5-1 μg of total RNA using the High Capacity cDNA Reverse Transcription kits (Life Technologies) following the manufacturer's instructions. TaqMan quantitative real-time PCR was performed using the following primers from Life Technologies: *Acp5* (Mm00475698_m1); *Bglap* (osteocalcin) (Mm03413826_mH); *CalcR* (Mm00432282_m1); *Ctsk* (Mm00484039_m1); *Def8* (Mm00459823_m1); *Fam98a* (Mm01223835_m1); *Ndel1* (Mm00502730_m1); *Nfatc1* (Mm00479445_m1); *Plekhm1* (Mm00805593_m1); *Runx2* (Mm00501584_m1). Samples were amplified using the StepOne^{Plus} real-time PCR system (Life Technologies) with an initial denaturation at 95 ºC for 10 min, followed by 40 cycles of 95 ºC for 15 s and 60 ºC for 1 min. The relative cDNA amount was calculated by normalizing to that of the mitochondrial gene Mrps2, which is steadily expressed in both BMMs and osteoclasts, using the ΔCt method.

DNA isolation and gene copy number determination

Soft tissues, tibiae and vertebrae were collected from three mice/genotype. The osteocyte enriched cortical bone was prepared as following. The proximal and distal ends of tibia were cut off, bone marrow were flushed out completely, the periosteum was scraped away from bone surface. The remaining cortical bones were incubated in 14% ethylenediaminetetraacetic acid (EDTA) for 1 week. The genomic DNAs of the cells and tissues were purified using DNeasy Blood & Tissue kit (Quigen) according to the manufacture's protocol. The custom-designed Taqman assay primer of the exon 3 of murine *Plekhm1* was purchased from Thermo-Fisher Scientific. The gene copy number was normalized to murin transferrin receptor 1 locus (Thermo-Fisher).

Western blotting

Cultured cells were washed with ice-cold PBS twice and lysed in 1 x RIPA buffer (R-0278, Sigma) containing 1 mM DTT and Complete Mini EDTA-free protease inhibitor cocktail (04693159001, Roche). After incubation on ice for 30 min, the cell lysates were clarified by centrifugation at 14,000 rpm for 15 min at 4°C. Ten to thirty μg of total protein were subjected to 8% or 10% SDS-PAGE gels and transferred electrophoretically onto polyvinylidene difluoride membrane (IPVH00010, EMD Millipore) by a semi-dry blotting system (Bio-Rad). The membrane was blocked in 5% fat-free milk/Tris-buffered saline for 1 hour and incubated with primary antibodies at 4°C overnight followed by secondary antibodies conjugated with horseradish peroxidase (Santa Cruz Biotechnology). After rinsing 3 times with Tris-buffered saline containing 0.1% Tween 20, the membrane was subjected to western blot analysis with enhanced chemiluminescent detection reagents (WBKLS0100, EMD Millipore).

Immunoprecipitation

Protein G magnetic beads (S1430, New England BioLabs) were pre-coated with mouse monoclonal anti-HA or anti-FLAG antibodies at 5μg antibody/20μl beads in lysis buffer [20mM Tris, 120mM NaCl, 1mM EDTA, 1mM EGTA, 2.5mM Sodium Pyrophosphate, 0.5% NP-40, 1 × Complete Mini EDTA-free protease inhibitor cocktail and 1 × Halt phosphatase inhibitor cocktail (#1862495, Thermo-Fisher Scientific)] at 4°C for 2 hours with rotation. The beads were washed three times with lysis buffer and added into 293-T or osteoclast cell lysates.

Lysates were incubated at 4°C for one hour and washed three times with the washing buffer (the lysis buffer with 0.2% NP-40). The beads were boiled in 2x SDS sample buffer for 5 min. Proteins were separated by 8 or 10% SDS-PAGE gels.

Immunofluorescence and laser confocal scanning microscopy

For staining of LAMP-2, cells were fixed with 4% paraformaldehyde in PBS for 20 min. None-specific binding was blocked by PBS/0.2% BSA/0.1% Saponin (PBSBS) for 30 min, followed by incubation with rat monoclonal anti-LAMP-2 antibody (GL2A7) in PBSBS for 1 hour. For EEA1 labeling, cells were fixed and penetrated at −20°C with methanol for 5 minutes and acetone for 30 s, followed by blocking with PBS/0.2% BSA for 30 min. Cells were then incubated with polycolonal or monoclonal anti-EEA1 (Supplementary Table3) in PBS/0.2% BSA for 1 hour. For rest of immunofluorescent staining, cells were fixed with 4% paraformaldehyde in PBS for 20min and permeabilized with 0.1% Triton X-100/PBS for 10min. None-specific binding was blocked by PBS/0.2% BSA for 30min. The primary antibodies (Supplementary Table3) were incubated in PBS/0.2% BSA for 1 hour. After three times 5-min-wash, cells were incubated with the respective fluorescent labeled secondary antibodies (Jackson ImmunoResearch Laboratories) for 45min. Samples were mounted with 90% glycerol/PBS. Immunofluorescence-labeled cells cultured on glass coverslips were observed under a Zeiss AxioImager Z1 fluorescent microscope equipped with Zeiss AxioCam MRm monochromatic and MR5c color cameras and a set of fluorescent filters. The images were acquired with Zeiss Axiovison 4.9 software. Osteoclasts cultured on bone slices were examined and analyzed using a Zeiss LSM 510 Meta laser confocal scanning microscope run by Zeiss Zen 2009 software.

Electron microscopy

Osteoclasts cultured on bovine bone slices were fixed with 5% glutaraldehyde in 0.16 M collidine buffer (pH 7.4) for 3 h. Bone slices were decalcified in 5% EDTA/0.1% glutaraldehyde for 3 days. Cells were postfixed in 2% OsO4/3% K-ferrocyanide for 2 h, dehydrated in ethanol, and embedded in Epon LX 112. Ultra-thin sections were stained briefly with lead citrate and examined using a FEI Technai F20 Transmission Electron Microscope equipped with FEI TEM Imaging & Analysis software.

Receptor degradation assay

Osteoclasts were cultured in 6-well plates with M-CSF and RANKL for 5 days. Cells were washed with PBS and incubated in serum-free α-MEM with 100ng/ml EGF (Life Technologies) or M-CSF (R&D). After 0min, 15min, 30min, 60min, and 120min of growth factor stimulation, osteoclasts were lysed with RIPA buffer and subjected to immune-blotting analysis.

Transferrin and Dextran pulse-chase experiments

Osteoclasts cultured on glass coverslips in a 24-well plate were washed with cold PBS and incubated in serum-free α-MEM with M-CSF and RANKL on ice for 15min to block endocytosis. 200nM human holo-Transferrin (T0665, Sigma-Aldrich) was added and cells were incubated on ice for 30min to allow Transferrin binding to Transferrin receptor on the plasma membrane. Cells were washed with cold medium. Osteoclasts were then incubated at 37°C for the indicated time-points before fixed by 4% paraformaldehyde in PBS for 20 min and processed for immunofluorescence.

Osteoclasts cultured in a 35mm culture dish were incubated with 0.5mg/ml Dextran tetramethylrhodamine (10,000MW, D-1868, Life Technologies) for 2 hours. Cells were washed three times and 35mm-dish was put into a Pathology Devices Live Cell stage insert set to 37°C, 5% CO_2, 80% Humidity. Live-cell imaging was captured using a Zeiss AxioObserver fluorescent microscope at 1min intervals for 2 hours.

Construction of vectors

The full-length murine *Plekhm1*, *Rab7* and LAMP-2a were amplified by PCR with specific primers (supplemental Figure 7) and Pfx DNA polymerase (Life Technologies) from a mature osteoclast cDNA library generated in our laboratory. The murine cDNAs encoding other proteins were amplified by PCR using the following templates purchased from Open Biosystems GE Dhamacon: Clasp2 (MMM1013-211693777), Def8 (MMM1013-202761163), Fam98a (MMM4769-202762410), KIFc1 (MMM1013-202761893), Map3k7 (Tak1, MMM1013-202762097), Ndel1 (MMM1013-202859039), Rap1b (MMM1013-202766273), Tpx2 (MMM1013-202859447). A series of mutants of *Plekhm1* were generated by PCR using pMX-BSR-*Plekhm1* as a template. Amplified

LAMP-2a was first cloned in-frame with GFP in a shuttle vector. The LAMP2a-GFP was then amplified by PCR. The amplified cDNAs were cloned into the pMX-IRES-BSR retrovirus vector. The sequences were verified by DNA sequencing.

Plasmid Transfection and Retro-/lenti-viral transduction

A total of 3μg of plasmids were transfected into 293-T cells (ATCC) in a 6-well culture dish using TransIT-LT1 transfect reagent (MIR2300, Mirus Bio LLC) and cells were cultured for 2-3 days. The recombinant retroviral vectors of full-length and mutant forms of Plekhm1 were transfected into Plat E retroviral packing cells (ATCC) using TransIT-LT1 transfection reagent. Virus supernatants were collected at 48 h after transfection. BMMs were transduced with viruses for 24 h in α-10 medium containing M-CSF and 20 μg/ml of protamine. Cells were then selected in α-10 medium containing M-CSF and 1.5 μg/ml of blasticidin (203350, EMD Chemicals) for 3 days.

The LKO.1 lentiviral vectors expressing shRNA sequence targeting specific mRNAs of were purchased from Sigma-Aldrich: murine Def8 [TRCN0000105902 (Def8-sh1) and TRCN0000105900 (Def8-sh2)], murine Ndel1 [TRCN0000178263 (Ndel1-sh1) and TRCN0000277513 (Ndel1-sh2)], murine Fam98a [TRCN0000283010 (Fam98a-sh1) and TRCN0000374721 (Fam98a-sh2]. A firefly luciferase shRNA was used as a control (5′-GCTTACGCTGAGTACTTCGA-3′). 293-T cells cultured in a 6-well culture dish were co-transfected with a total of 3μg of LKO.1 gene transfer vector and virus packaging vectors, ΔH8.2 and VSVG by TransIT-LT1 transfection reagent. Virus supernatants were collected after 48 hours transfection. BMMs were transduced with virus supernatant containing M-CSF and 20 μg/ml of Protamine (Sigma-Aldrich). Cells were then selected in α-10 medium containing M-CSF and 6 μg/ml puromycin (Sigma-Aldrich) for 3 days.

Time-lapse live cell imaging

For live-cell imaging, osteoclasts were cultured in a 35mm cell culture dish. The dish was put into a Pathology Devices Live Cell stage insert set to 37°C, 5% CO_2, 80% Humidity. Live-cell imaging was performed using a Zeiss AxioObserver fluorescent microscope equipped with Photometrics CoolSnap HQ camera and Definite Focus attachment for time-lapse stability. Images were recorded with Zeiss Axiovison 4.9 software at 1min

intervals for 2 hours. A total of 120 images in Zvi format were converted into Avi format at 7 frames/s with NIH ImageJ software.

Mass-spectrometry and proteomic analysis

Proteins were run on SDS-PAGE using NuPage Bis-Tris 4-12% gradient gels (Life Technologies) and stained with SimplyBlue Coomassie G-250 (Life Technologies). Each gel lane was sliced into 4 mm segments and subjected to in-gel trypsin digestion as follows. Gel slices were destained in 50% methanol (Fisher Scientific), 100 mM ammonium bicarbonate (Sigma-Aldrich), followed by reduction in 10 mM Tris[2-carboxyethyl]phosphine (Pierce) and alkylation in 50 mM iodoacetamide (Sigma-Aldrich). Gel slices were then dehydrated in acetonitrile (Fisher Scientific), followed by addition of 100 ng porcine sequencing grade modified trypsin (Promega) in 100 mM ammonium bicarbonate (Sigma-Aldrich) and incubation at 37^{o}C for 12-16 hours. Peptide products were then acidified in 0.1% formic acid (Pierce). Tryptic peptides were separated by reverse phase Jupiter Proteo resin (Phenomenex) on a 100 x 0.075 mm column using a nanoAcquity UPLC system (Waters). Peptides were eluted using a 40 min gradient from 97:3 to 35:65 buffer A:B ratio (Buffer A = 0.1% formic acid, 0.5% acetonitrile; buffer B = 0.1% formic acid, 75% acetonitrile). Eluted peptides were ionized by electrospray (1.9 kV) followed by MS/MS analysis using collision induced dissociation on an LTQ Orbitrap Velos mass spectrometer (Thermo Scientific). MS data were acquired using the FTMS analyzer in profile mode at a resolution of 60,000 over a range of 375 to 1500 m/z. MS/MS data were acquired for the top 15 peaks from each MS scan using the ion trap analyzer in centroid mode and normal mass range with a normalized collision energy of 35.0.

Proteins were identified by searching the UniProtKB SwissProt database (2014_02 release; restricted to *Mus musculus*; 16,656 entries) using an in-house Mascot Sever (v 2.4; Matrix Science). Peak lists were generated from raw data files by MSFileReader (v2.2; Thermo Scientific) and ExtractMSn (January 2011 release; Thermo Scientific). Charge state deconvolution and deisotoping were not performed. No contaminants were excluded from the data set. Mascot search parameters were specified as follows: trypsin digestion with up to two missed cleavages; fixed carbamidomethyl modification of cysteine; variable oxidation of methionine; variable N-terminal

acetylation; 2.0 ppm precursor ion tolerance; 0.50 Da fragment ion tolerance. A reverse-sequence decoy search was also performed. Peptide and protein identifications were validated using Scaffold (v4.3; Proteome Software). Peptide identifications were accepted at <1.0% false discovery as determined by the Scaffold Local FDR algorithm. Protein identifications were accepted at <1.0% false discovery and a minimum of two identified peptides. Protein probabilities were assigned by the Protein Prophet algorithm. Proteins with similar peptides that could not be differentiated based on MS/MS analysis alone were grouped to satisfy the principles of parsimony. Proteins sharing significant peptide evidence were grouped into clusters.

Micro-CT

The left femurs and L4 vertebrae were cleaned of soft tissues and fixed in 10% Millonig's formalin with 0.5% sucrose for 24 hours. The bone samples were gradually dehydrated into 100% ethanol. The bones were loaded into a 12.3-mm diameter scanning tube and were imaged in a μCT (model μCT40, Scanco Medical).We integrated the scans into 3-D voxel images (1024 x 1024 pixel matrices for each individual planar stack) and used a Gaussian filter (sigma = 0.8, support = 1) to reduce signal noise. A threshold of 200 was applied to all scans, at medium resolution (E = 55 kVp, I = 145 μA, integration time = 200ms).

Histology and bone histomorphometry

30μg of Tetracycline per gram of mouse weight was injected into mice at day 8 and day4 prior to sacrifice. The femurs were fixed in 10% Millonig's formalin with 0.5% sucrose for 24 h and were gradually dehydrated into 100% ethanol.The left femurs were embedded undecalcified in methyl methacrylate and stained for Toluidine blue. The static and dynamic histomorphometric examination of trabecular bone was done on 5 μm longitudinal sections with a digitizer tablet (OsteoMetrics, Inc., Decatur, GA, USA) interfaced to a Zeiss Axioscope (Carl Zeiss, Thornwood, NY, USA) with a drawing tube attachment. The right femurs were fixed in 10% Millonig's formalin for 24 h and were decalcified in 14% EDTA for 7-10 days. The bones were embedded in paraffin before obtaining 5-μm longitudinal sections. After removal of paraffin and rehydration, sections were stained for TRAP activity and counter-stained with methyl green and osteoclasts were enumerated on the trabecular bone surface.

Supplemental Figures

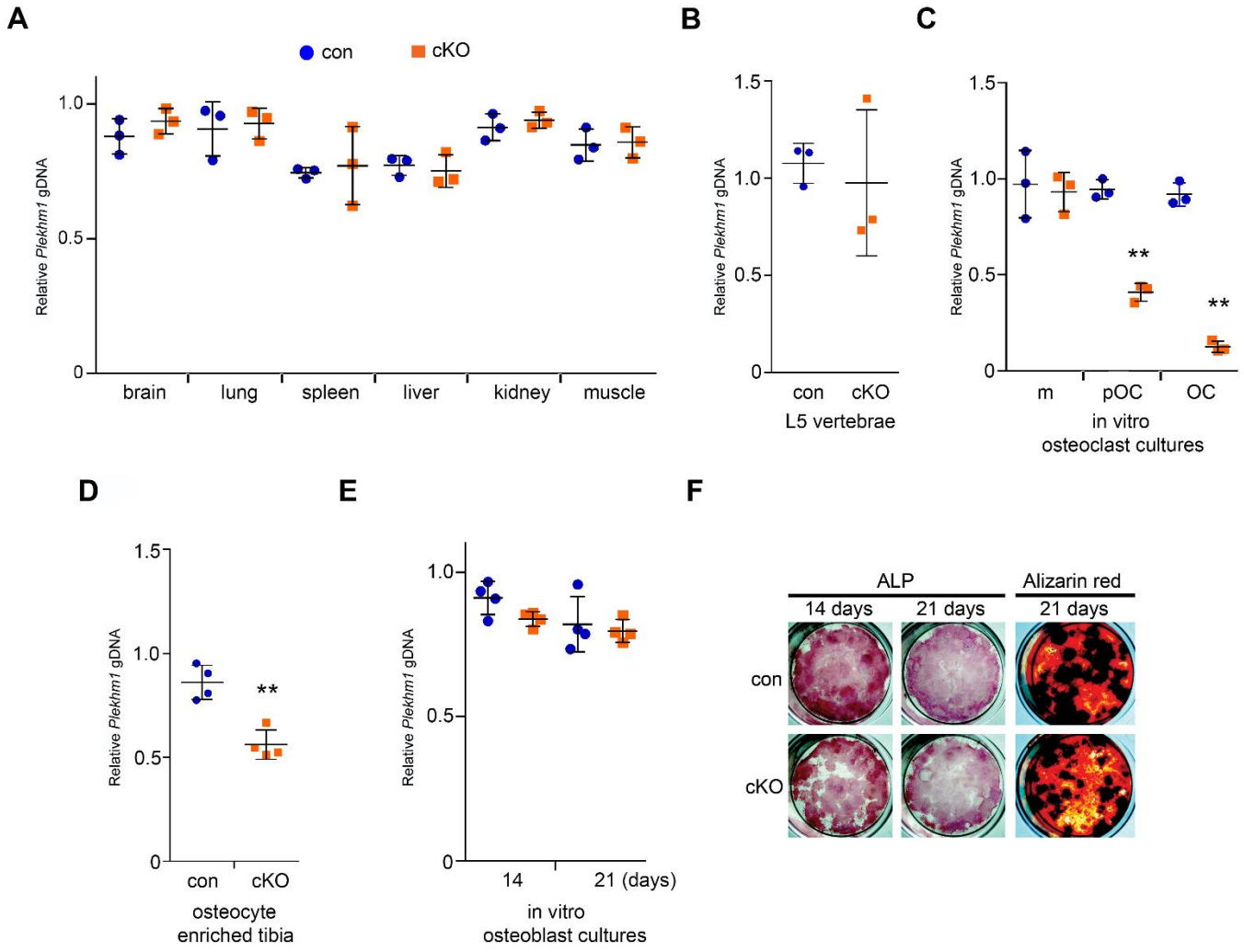

Figure 1. Deletion of murine *Plekhm1* genomic DNA by *Ctsk*-Cre. Quantitative PCR of the exon 3 of murine *Plekhm1* genomic DNA, normalized to the transferrin receptor 1 locus, using genomic DNA isolated from the indicated soft tissues (n = 3) (A), number 5 lumber (L5) vertebrae (n = 3) (B), in vitro cultured osteoclast lineage cells (n = 3) (C), osteocyte-enriched tibia cortical bone (n = 4) (D), and osteoblasts from 14- and 21-day cultures of bone marrow stromal cells (n = 4) (E). Data in (A) to (E) are presented as scatter dot plots. The mean and standard deviation of each group are overlaid onto each column of dots. con, control; cKO, conditional knockout; m, bone marrow monocytes; pOC, pre-osteoclasts; OC, mature osteoclasts. ** in (C), $p < 0.01$ versus con by one way ANOVA. ** in (D), $p < 0.01$ versus con by Student's t-test. (F) Alkaline phosphatase (ALP) and Alizarin red bone nodule staining of 14- and 21-day cultures of osteoblasts from bone marrow stromal cells in a 12-well culture plate. Original magnification: 1 ×.

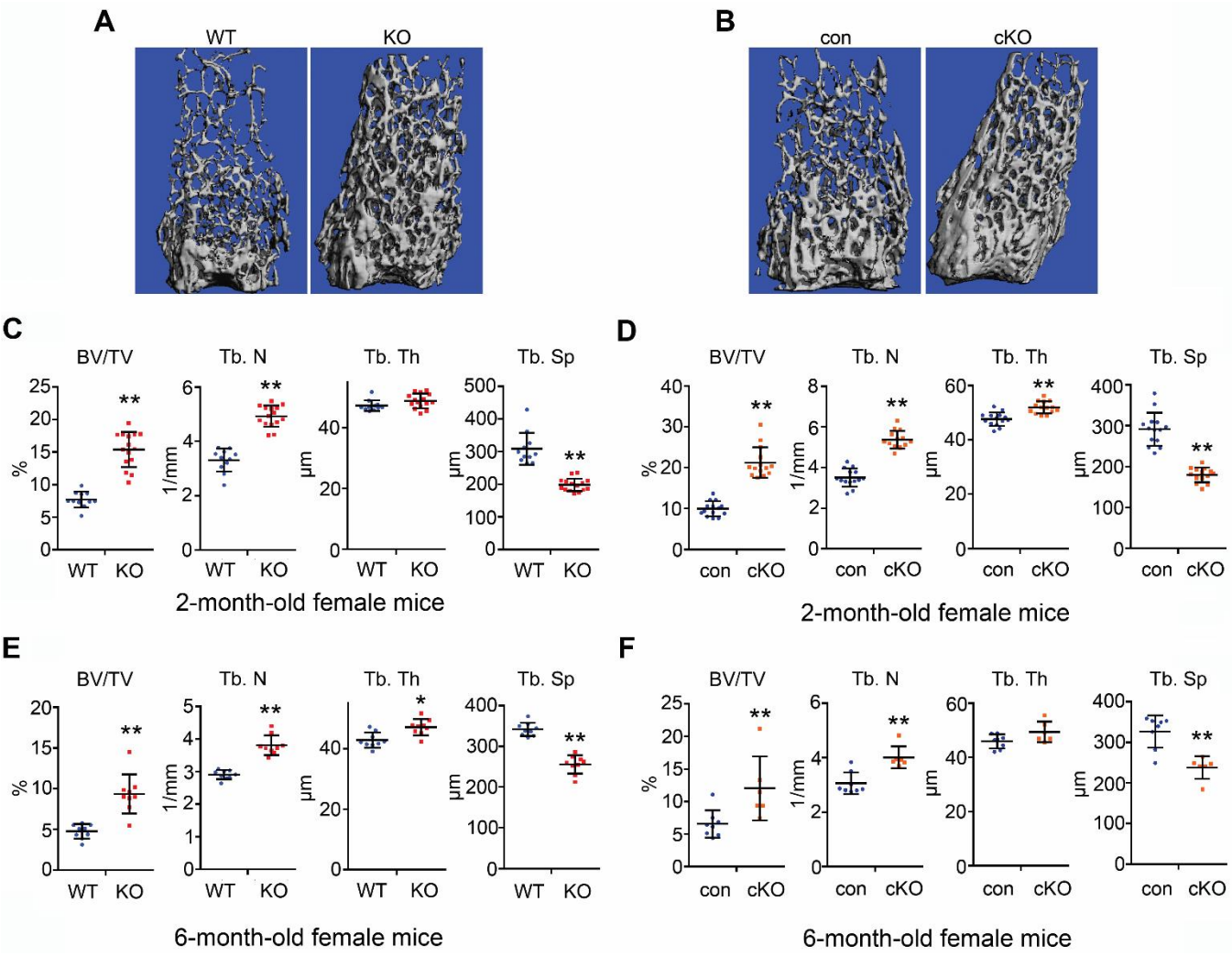

Figure 2. *Plekhm1* germline and conditional deficient female mice have increased trabecular bone mass at 2- and 6-month old of age. (A) and (C) µ-CT images and analyses of trabecular bone compartment of the distal femurs of 2-month-old female wild type (WT) and *Plekhm1*$^{-/-}$ (KO) mice (n: WT = 11, KO = 15). (B) and (D) µ-CT images and analyses of trabecular bone compartment of the distal femurs of 2-month-old female control (con) and *Plekhm1* conditional deletion (cKO) mice (n: con = 14, KO = 14). (E) and (F) µ-CT analyses of trabecular bone compartment of the distal femurs of 6-month-old female mice (n: WT = 9, KO = 9; con = 8, cKO = 6). BV/TV, percentage of trabecular bone volume to tissue volume; Tb. N, trabecular number; Tb. Th, trabecular thickness; Tb.Sp, trabecular separation. Data in (C) to (F) are presented as scatter dot plots. The mean and standard deviation of each group are overlaid onto each column of dots.** $p < 0.01$; * $p < 0.05$, versus WT or con by Student's t-test.

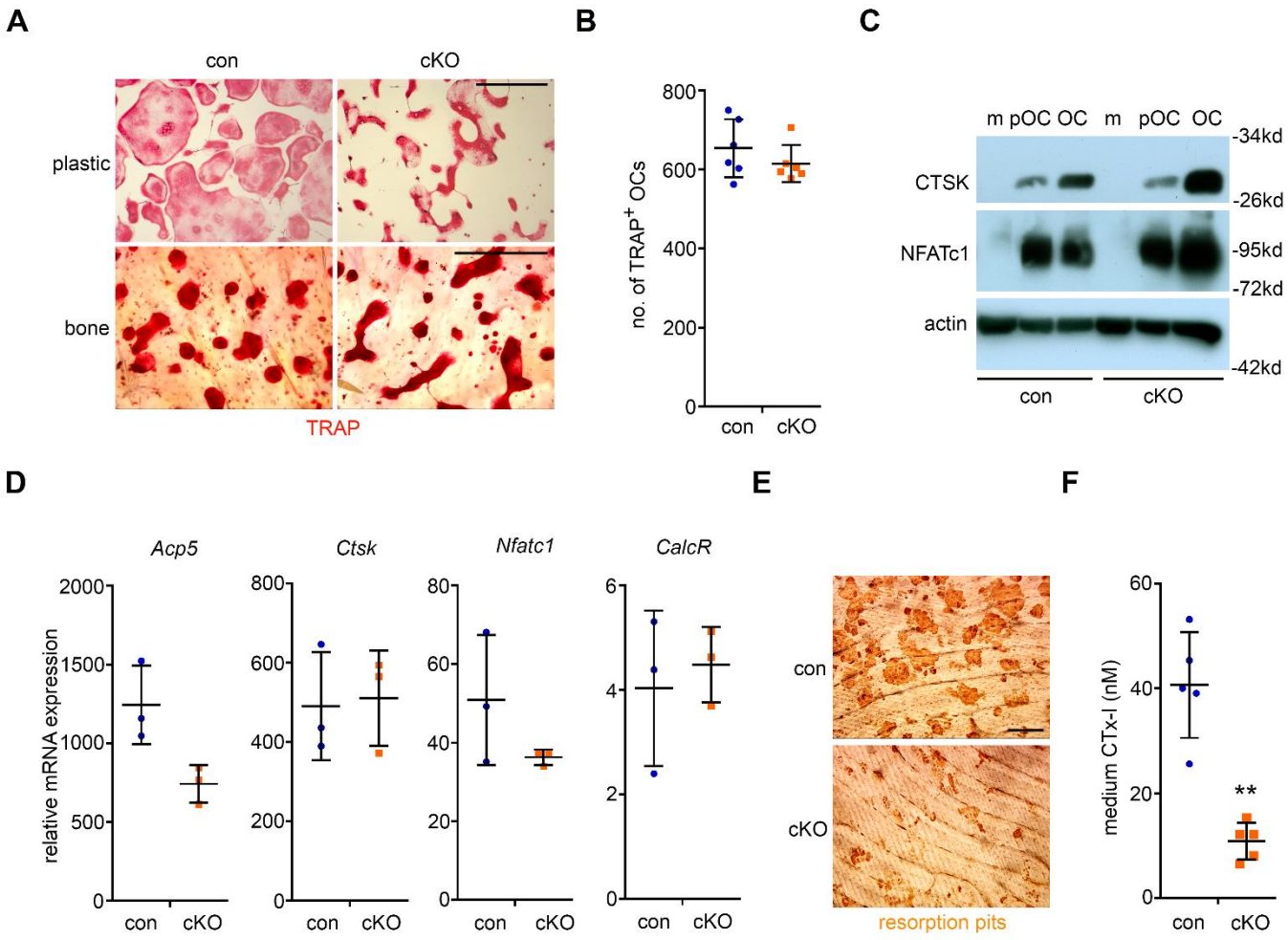

Figure 3. Loss of *Plekhm1* in osteoclasts attenuates bone resorption without affecting osteoclast differentiation. (A) Tartrate-resistant acid phosphatase (TRAP) straining of control (con) and *Plekhm1* conditional knockout (cKO) osteoclasts cultured on plastic dishes and bovine cortical bone slices. Representative images are from 6 samples/group/culture of three independent cultures from different mice. Scale bar = 200μm. (B) Number of $TRAP^+$ osteoclasts with more than three nuclei per well of 48-well plate (n = 6). (C) Protein expression of osteoclast markers, CTSK (cathepsin K) and NFATc1 (nuclear factor of activated T-cells, cytoplasmic 1), detected by western blotting during osteoclast differentiation. Actin served as a loading control. m, bone marrow monocytes; pOC, pre-osteoclasts; OC, mature osteoclasts. The experiment was repeated three times. (D) mRNA expression of osteoclast marker genes in mature osteoclasts measured by quantitative real-time PCR. *Acp5* (TRAP); *Ctsk; Nfactc1; CalcR* (calcitonin receptor) (n = 3). (E) Resorption pit staining of con and cKO osteoclasts cultured on bone slices. Each image is a representative of 6 bone slices/group/culture from at least three independent cultures from different mice. Scale bar = 40μm. (F) The amount of medium CTx-I, collagen fragments released by osteoclasts during bone resorption, was measured by ELISA (n = 5). The data in (B), (D), and (F) are presented as scatter dot plots. The mean and standard deviation of each group are overlaid onto each column of dots.** $p < 0.01$ versus con by Student t-test.

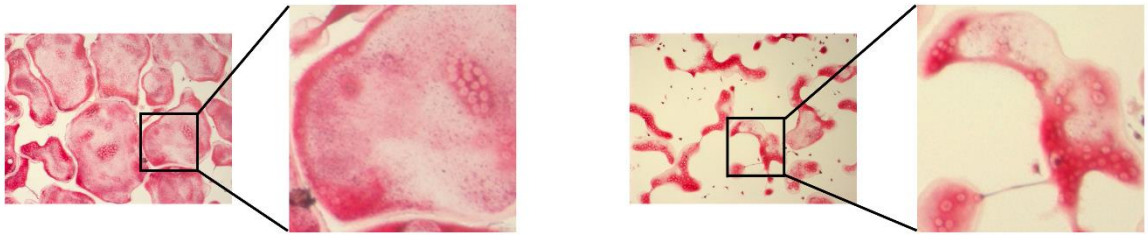

Figure 4. Enlarged images of TRAP-stained wild type (WT) and *Plekhm1* knockout (KO) osteoclasts.

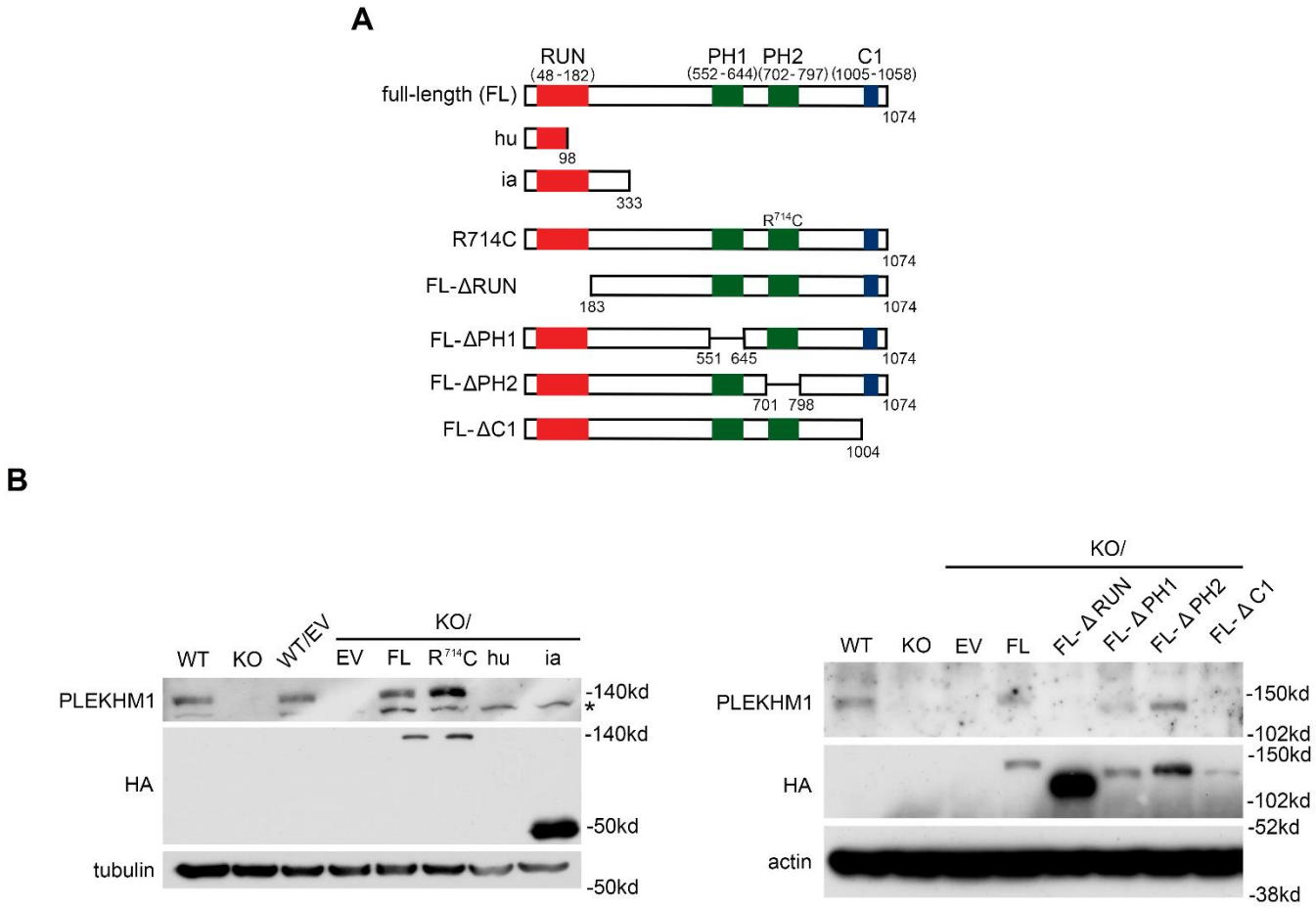

Figure 5. Protein expression of endogenous and HA tagged PLEKHM1 in osteoclasts. (A) Schematic illustration of the structural domains of full-length (FL) and mutants of PLEKHM1. Numbers indicate positions of amino acids. (B) Western blot detection of endogenous and reconstituted HA tagged FL and mutants of PLEKHM1. EV, empty vector. *, unspecific band. Tubulin and actin served as loading controls.

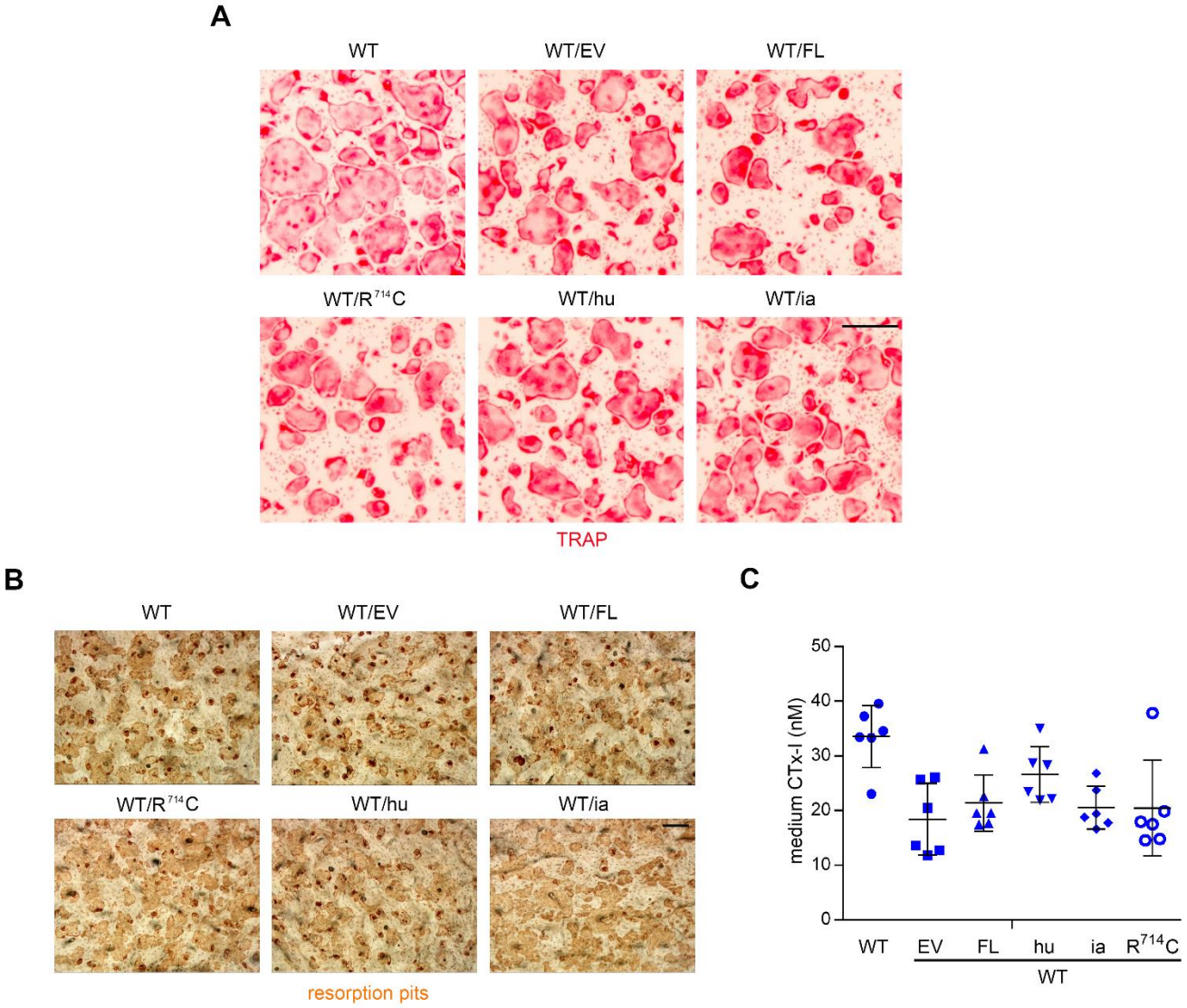

Figure 6. Retroviral transduction of PLEKHM1 mutants in wild type bone marrow monocytes has no effects on osteoclast differentiation and function. (A) TRAP staining of wild type osteoclasts expressing the empty vector (EV), the full-length (FL), the human and ia rat mutants (see supplemental Figure 5A). Scale bar = 200μm. (B) resorption pit staining. Scale bar = 40μm. (C) The amount of medium CTx-I measured by ELISA. The data are presented as scatter dot plots. The mean and standard deviation of each group are overlaid onto each column of dots. The experiments were repeated twice.

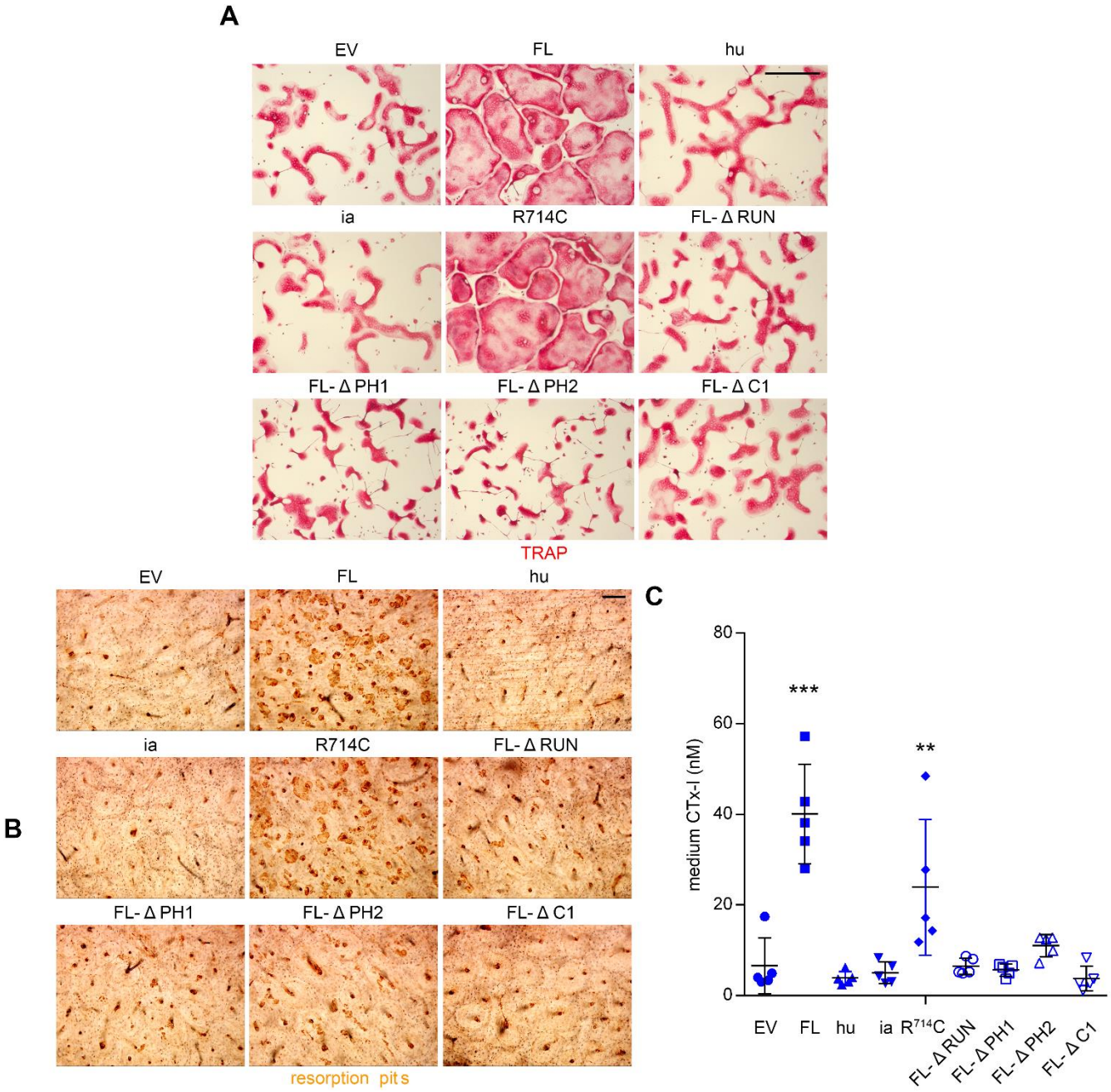

Figure 7. PLEKHM1 plays an intrinsic role in osteoclast function. (A) TRAP staining of *Plekhm1*$^{-/-}$ osteoclasts retrovirally transduced with the empty vector (EV), the full-length (FL) or different mutants (see supplemental Figure 5A) of murine PLEKHM1. Scale bar = 100μm. (B) Resorption pit staining. Scale bar = 40μm. The experiments in (A) and (B) were repeated at least three times using cells isolated from different mice. (C) The amount of medium CTx-I measured by ELISA (n = 6). The data are presented as scatter dot plots. The mean and standard deviation of each group are overlaid onto each column of dots. *** $p < 0.001$, ** $p < 0.01$ versus EV transduced osteoclasts by one-way ANOVA.

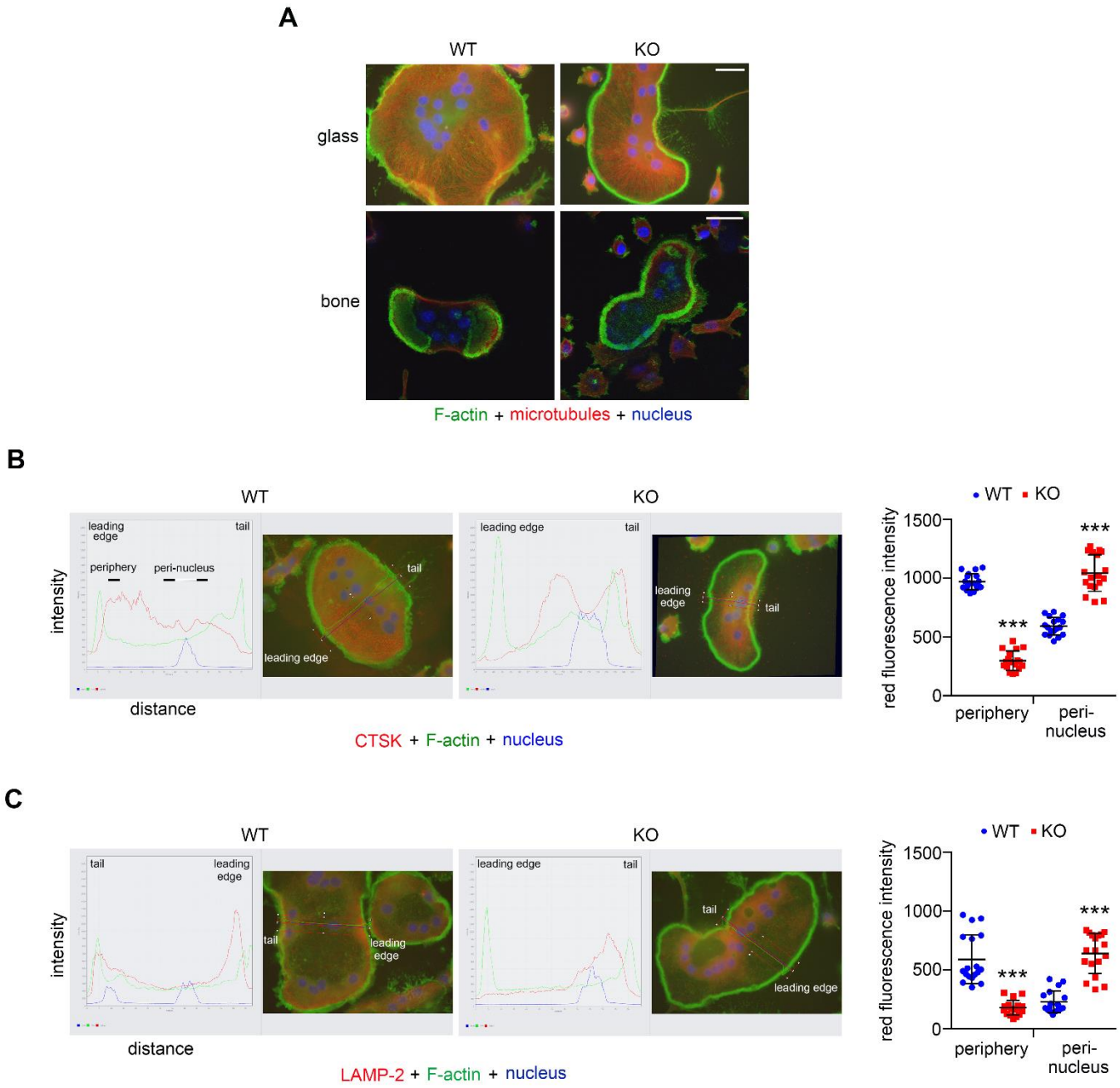

Figure 8. PLEKHM1 regulates lysosome peripheral distribution but not cytoskeleton organization in osteoclasts. (A) Immunofluorescent staining of filamentous actin (F-actin), microtubules, and nucleus in wild type (WT) and *Plekhm1*$^{-/-}$ (KO) osteoclasts cultured on glass coverslips (upper panels) and bone slices (lower panels). Representative images are from 6 samples/group/culture of three independent cultures from different mice. (B) and (C) Quantifications of lysosome distribution at the cell periphery and the peri-nuclear regions in immunofluorescence-stained cathepsin K (CTSK) and LAMP-2 of WT and KO osteoclasts using Zen 2.0 Blue Profile View software (Zeiss). A quantification line (the middle purple line) was drawn from the leading edge to the tail around the middle of osteoclasts. The red fluorescent intensities along 5-µm inside the podosome-belt (green peak) at the leading edge (periphery) and 5-µm surround the nucleus (peri-necleus) in osteoclasts, shown in black bars, were quantified by the software. The data are presented as scatter dot plots (n = 18). The mean and standard deviation of each group are overlaid onto each column of dots. *** $p < 0.001$ versus WT by one-way ANOVA. The analysis was performed in a double-blinded manner.

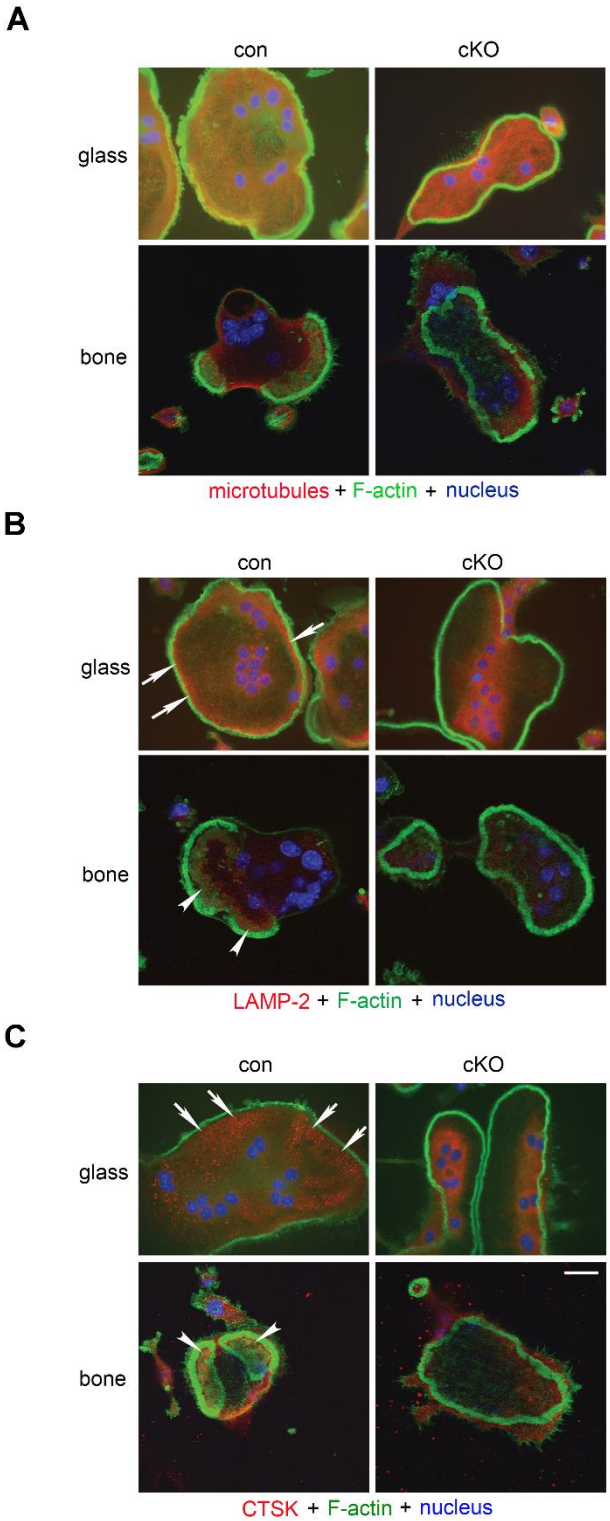

Figure 9. Deletion of *Plekhm1* in osteoclasts by *Ctsk*-Cre inhibits lysosome peripheral distribution but not cytoskeleton organization. (A) Immunofluorescent staining of filamentous actin (F-actin), microtubules, and nucleus in osteoclasts cultured on glass coverslips (upper panels) and bone slices (lower panels). (B) Immunofluorescent staining of F-actin, LAMP-2, and nucleus in osteoclasts cultured on glass coverslips (upper panels) and bone slices (lower panels). White arrows in upper panels point out the distribution of LAMP-2 positive lysosomes at the periphery of control osteoclasts cultured on glass coverslips. White arrow heads in the lower panels point out the localization of LAMP-2 at the ruffled border of control osteoclasts cultured on bone slices. (C) Immunofluorescent staining of F-actin, CTSK (cathepsin K), and nucleus in osteoclasts cultured on glass coverslips (upper panels) and bone slices (lower panels). White arrows in upper panels point out the spreading distribution of CTSK in wild type osteoclasts cultured on glass coverslips. White arrow heads in the lower panels point out the secretion of CTSK in the resorption lacuna of control osteoclasts cultured on bone slices. Representative images are from 6 samples/group/culture of three independent cultures from different mice. Scale bar = 20μm.

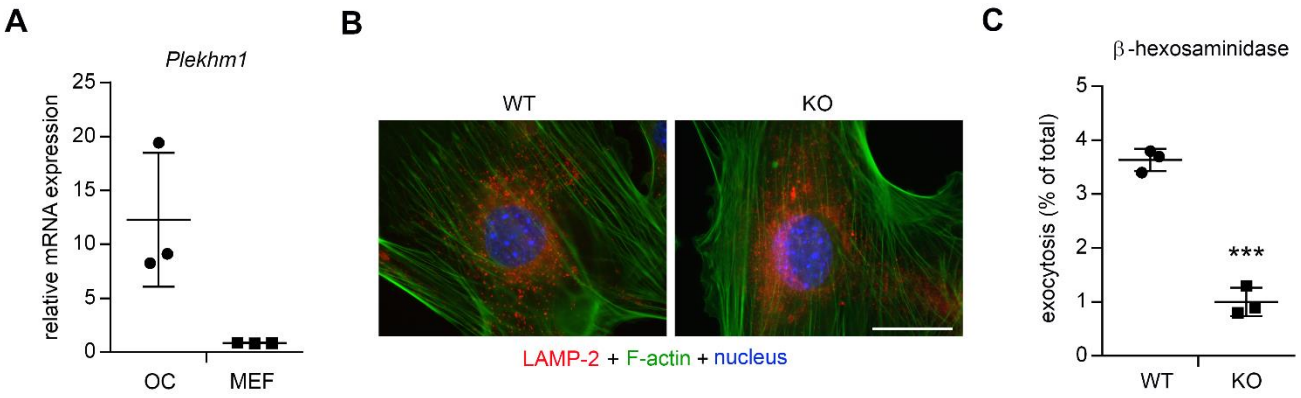

Figure 10. Loss of PLEKHM1 inhibits lysosome exocytosis in mouse embryonic fibroblasts. (A) mRNA level of *Plekhm1* in osteoclasts (OC) and mouse embryonic fibroblasts (MEF) detected by qPCR. (n = 3). (B) Immunofluorescent staining of LAMP-2 in MEFs. Scale bar = 10 μm. (C) regulated exocytosis of lysosomes, as assayed by the release of beta-hexoaminidase in streptolysin-O permeabilized MEFs. (n = 3). The data in (A) and (C) are presented as scatter dot plots. The mean and standard deviation of each group are overlaid onto each column of dots. *** $p < 0.001$ versus WT by Student t-test. The experiments was repeated three times.

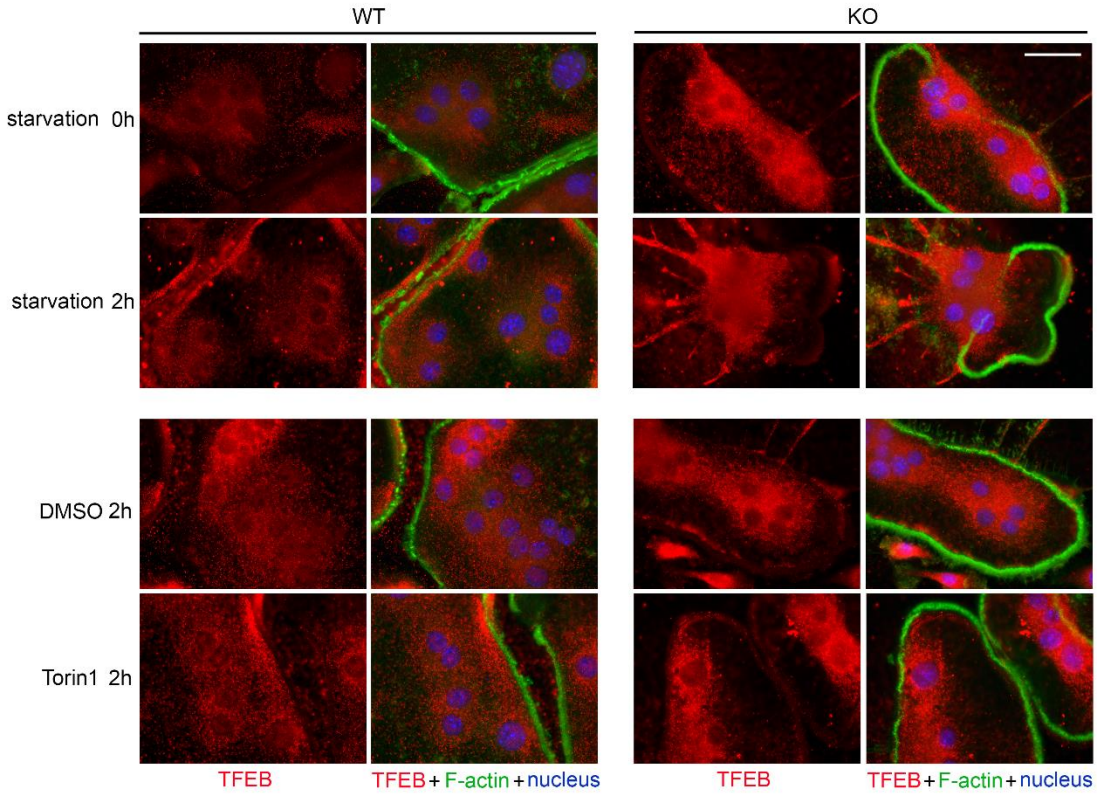

Figure 11. Starvation and treatment of mTOR inhibitor Torin1 in mature osteoclasts do not induce dramatic nuclear translocation of TFEB. Wild type and *Plekhm1*$^{-/-}$ mature osteoclasts cultured on glass coverslips were under serum and amino acid starvation in HBSS buffer for 2 hours or treated with either DMSO or 250nM Torin1 for 2 hours. The distribution of TFEB was examined by immunofluorescence using a goat anti-TFEB antibody (Thermo-Fisher Scientific). Scale bar = 20μm. The experiment was repeated twice.

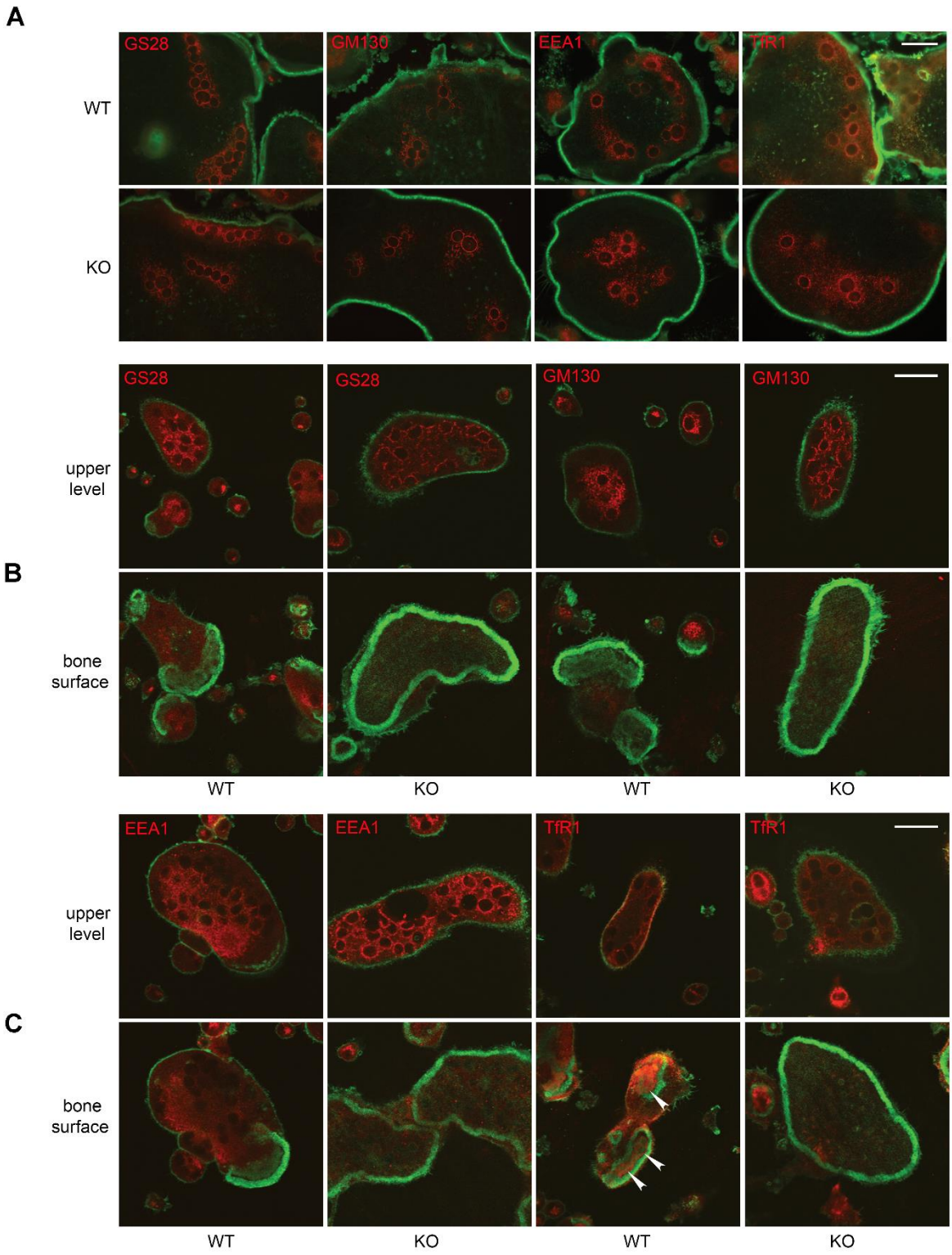

Figure 12. The distribution of Golgi apparatus, early endosomes, and recycling endosomes is not affected by loss of *Plekhm1* in osteoclasts. (A) Immunofluorescent staining of Golgi markers (GS28 and GM130), early endosome marker (EEA1), and recycling endosome marker (transferrin receptor, TfR1) in wild type (WT) and *Plekhm1*$^{-/-}$ (KO) osteoclasts cultured on glass coverslips. Scale bar = 20μm. (B) immunofluorescent staining of GS28 and GM130 in osteoclasts cultured on bone slices. Scale bar = 20μm. (C) immunofluorescent staining of EEA1 and endocytosed human holo-transferrin in osteoclasts cultured on bone slices. White arrow heads point out the accumulation of transferrin in the resorption lacuna. Scale bar = 20μm.

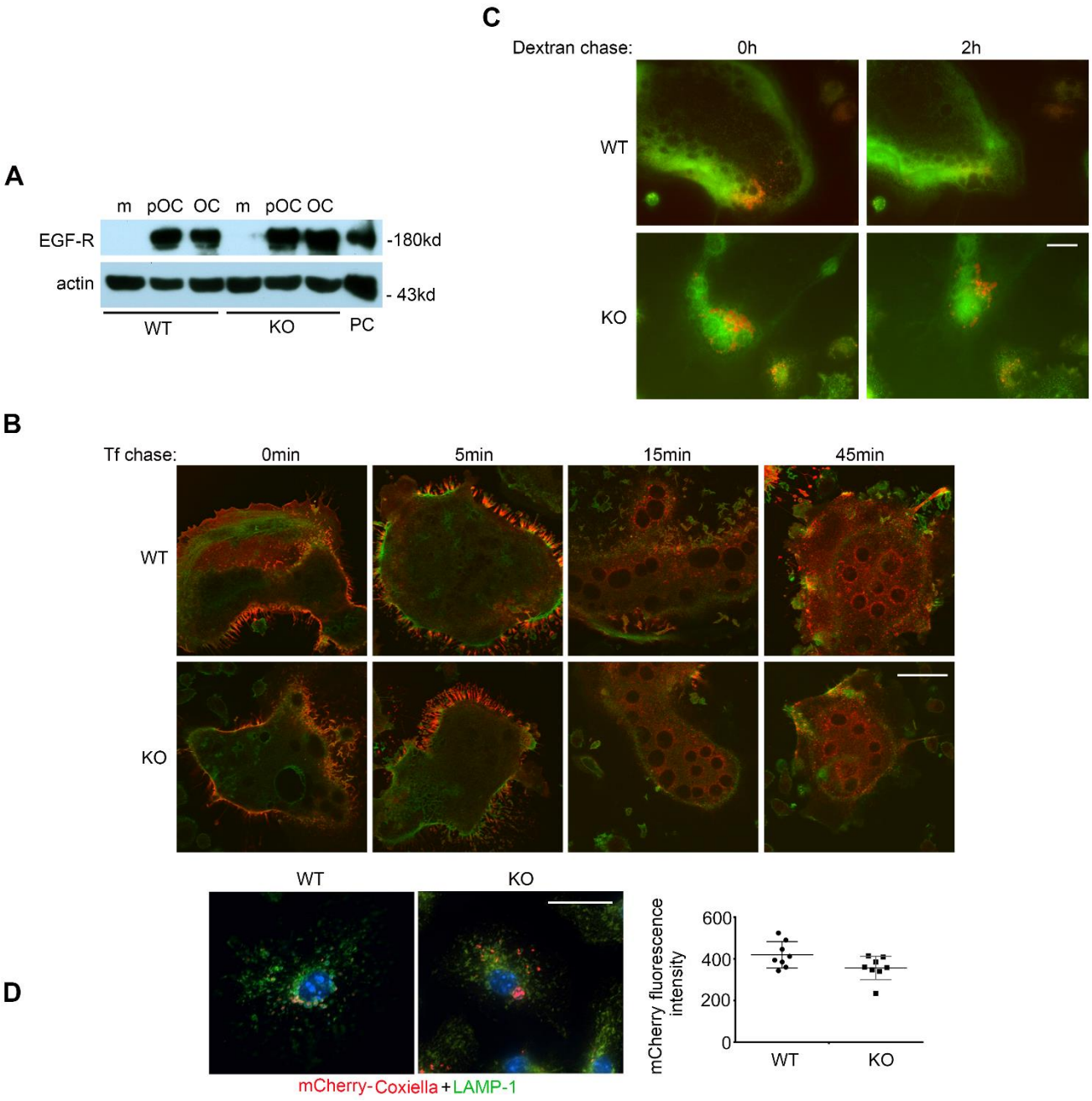

Figure 13. Loss of *Plekhm1* has no effects on EGF receptor (EGF-R) expression and endocytosis/phagocytosis in osteoclasts. (A) Western blot detection of EGF-R protein expression during osteoclast differentiation in wild type (WT) and *Plekhm1*-deficient (KO) cultures. m, bone marrow monocytes; pOC, pre-osteoclasts; OC, mature osteoclasts; PC, positive control. (B) Pulse-chase of human holo-transferrin, a receptor-mediated endocytosis marker, in osteoclasts cultured on glass coverslips. Scale bar = 20μm. (C) Pulse-chase of Alexa fluor 568 labeled Dextran (molecular weight 10,000MW, Thermo-Fisher Scientific), a fluid-phase endocytosis marker, in LAMP-2-GFP expressing osteoclasts. Scale bar = 20μm. (D) Immunofluorescent staining and quantification of phagocytosed mCherry-labeled Coxiella and LAMP-1 in macrophages. Scale bar = 20μm. The right panel represents scatter dot plots (n = 8) of 3 different cultures. The mean and standard deviation of each group are overlaid onto each column of dots.

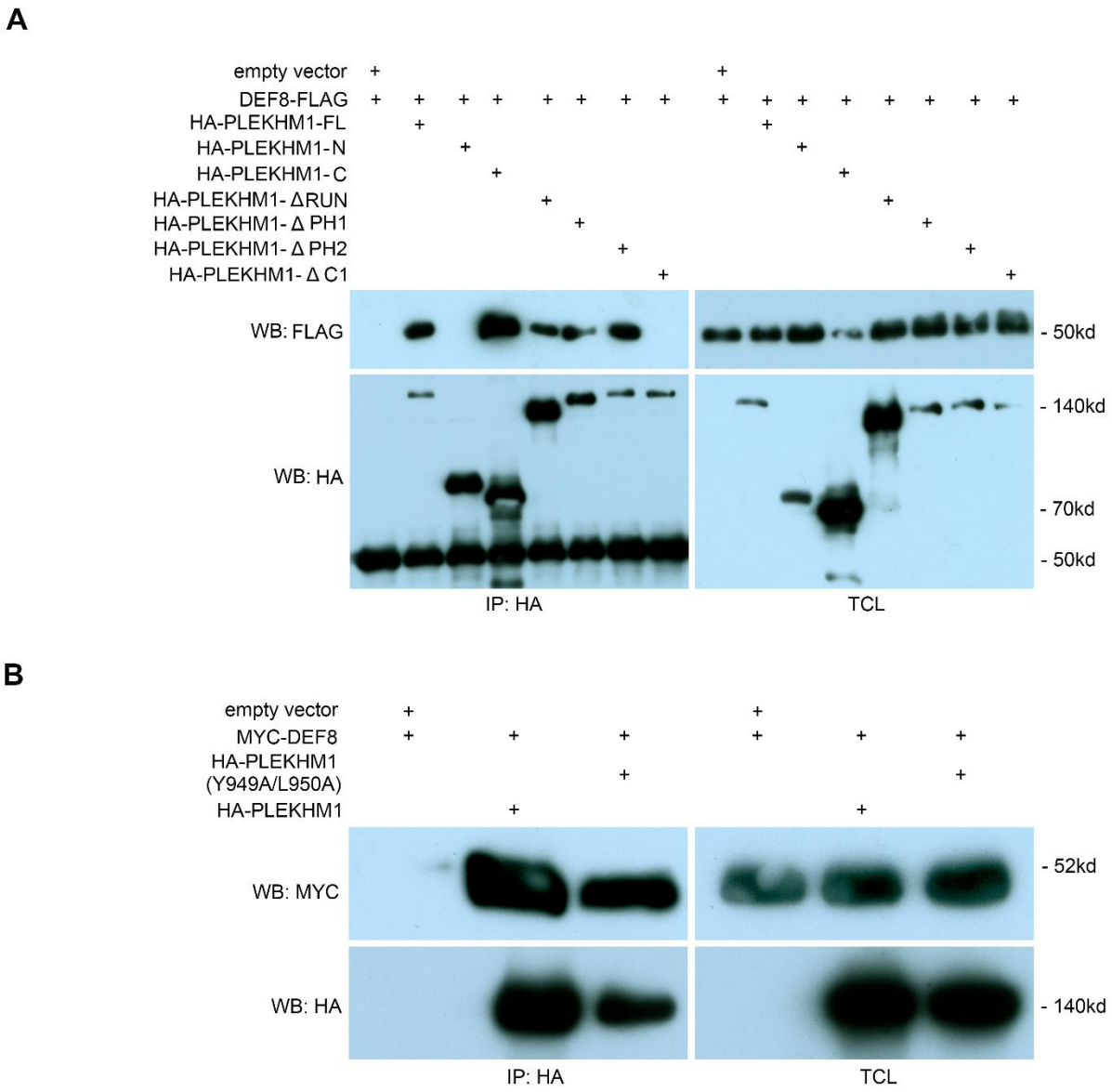

Figure 14. The C-terminal region of PLEKHM1 mediates its binding to DEF8. (A) co-immunoprecipitation of HA tagged full-length (FL) and a series of deleting mutants (see supplemental Figure 5A) of PLEKHM1 with FLAG tagged DEF8 in 293-T cells. The lysate of empty vector expressing cells served as a negative control. (B) co-immunoprecipitation of HA tagged PLEKHM1 or PLEKHM1 with Y949A/L950A double mutations at the RH domain with MYC tagged DEF8 in 293-T cells. The lysate of empty vector expressing cells served as a negative control. The experiments were repeated three times.

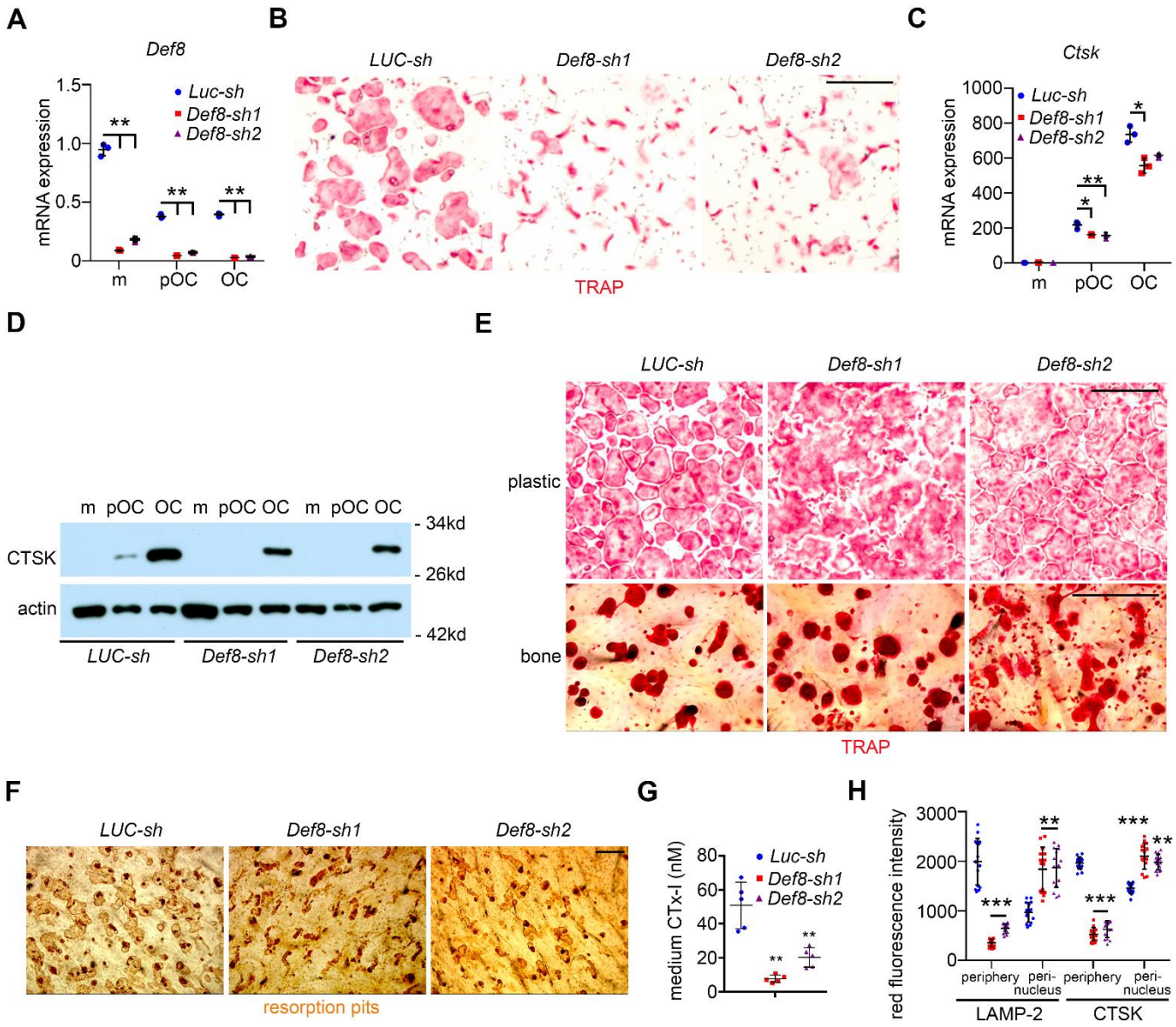

Figure 15. Loss of *Def8* mRNA expression in bone marrow monocytes in vitro inhibits osteoclast formation, lysosome peripheral distribution, and bone resorption. (A) qPCR detection of *Def8* mRNA levels in control (*LUC-sh*) and *Def8* shRNA (*Def8-sh1* and *Def8-sh2*) expressing bone marrow monocytes (m), pre-osteoclasts (pOC), and mature osteoclasts (OC) (n = 3). ** $p < 0.01$ versus *LUC-sh* by one-way ANOVA. (B) TRAP staining of control and *Def8* knocking-down osteoclasts (at the density of 1.5×10^4 monocytes/well of a 48-well culture plate). Scale bar = 200μm. Representative images are from 6 samples/group/culture of three independent cultures. (C) qPCR detection of cathepsin K (*Ctsk*) mRNA expression in control and *Def8* knocking-down osteoclast lineage cells (n = 3). * $p < 0.05$, ** $p < 0.01$ versus *LUC-sh* by one-way ANOVA. (D) CTSK protein expression in control and *Def8* knocking-down osteoclast lineage cells detected by western blots. Actin served as a loading control. (E) TRAP staining of control and *Def8* knocking-down osteoclasts cultured on plastic culture dishes (upper panels) or cortical bovine bone slices (lower panels) with increasing cell density (4.5×10^4 monocytes/well of a 48-well culture plate). Scale bars = 200μm. (F) Resorption pit staining of osteoclasts cultured in (E). Scale bar = 40μm. (G) medium CTx-I level of cultures in (E) measured by ELISA (n = 5). ** $p < 0.01$ versus *LUC-sh* by one-way ANOWA. (H) Quantifications of lysosome distribution at the cell periphery and the peri-nuclear regions in immunofluorescence-stained LAMP-2 and CTSK in control and *Def8*-knocking-down osteoclasts (n = 15) cultured on glass coverslips using Zen 2.0 Blue Profile View software (Zeiss). See figure legend of the supplemental Figure 8B-8C for the detailed methodology. ** $p < 0.01$, and *** $p < 0.001$ versus *LUC-sh* expressing osteoclasts by one-way ANOVA. Data in (A), (C), (G), and (H) are presented as scatter dot plots. The mean and standard deviation of each group are overlaid onto each column of dots.

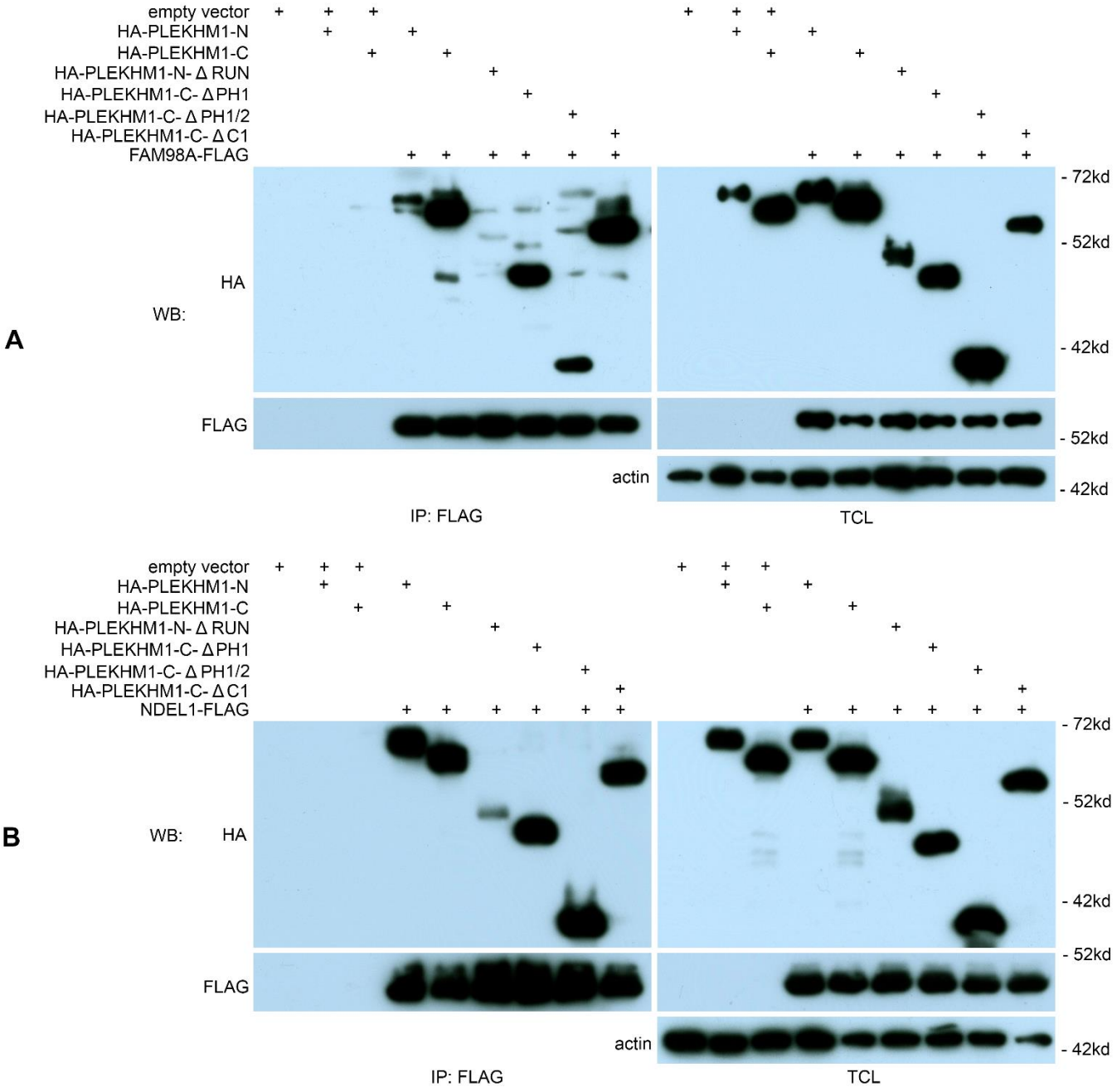

Figure 16. Interactions of FAM98A and NDEL1 with a series of PLEKHM1 fragments. Co-immunoprecipitations (IP) of FLAG tagged FAM98A (A) and NDEL1 (B) with a series of HA tagged PLEKHM1 fragments in 293-T cells. The lysates of 293-T cells expressing the empty vector alone (lane 1) or empty vector + HA-PLEKHM-N (lane 2), or empty vector + HA-PLEKHM1-C (lane 3) served as negative controls. Actin, served as loading controls. TCL, total cell lysate. The experiments were repeated three times

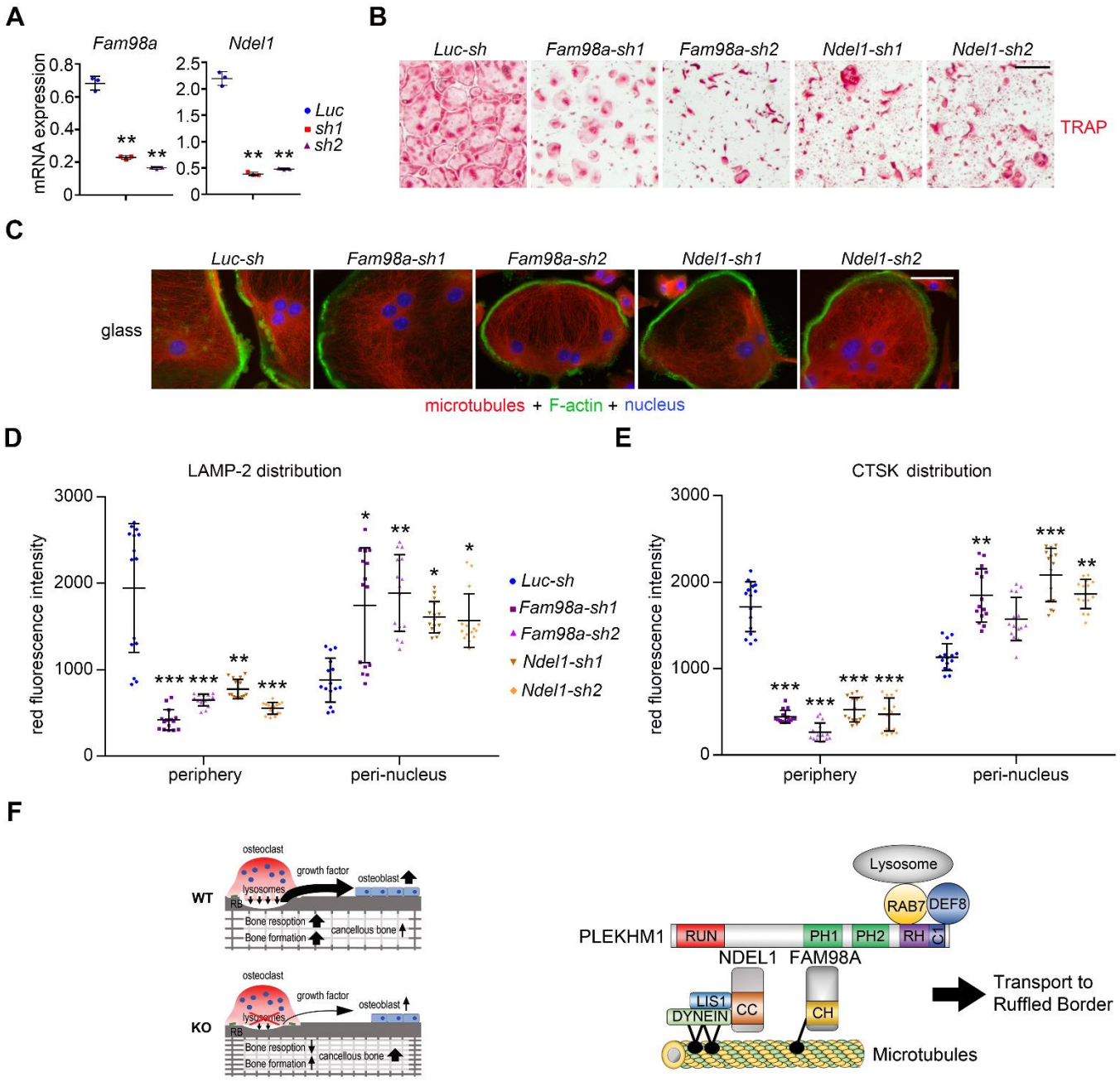

Figure 17. Depletion of *Fam98a* and *Ndel1* mRNA expression in bone marrow monocytes in vitro inhibits osteoclast formation and lysosome peripheral distribution but not cytoskeleton organization. (A) qPCR detection of *Fam98a* and *Ndel1* mRNA levels in control (*LUC-sh*) and two specific shRNAs (*sh1 and sh2*) expressing osteoclasts (n = 3). ** $p < 0.01$ versus *LUC-sh* by one-way ANOVA. (B) TRAP staining of control and *Fam98a*-, *Ndel1*-knocking-down osteoclasts cultured on plastic. Scale bar = 200µm. (C) Immunofluorescent staining of microtubules, filamentous actin (F-actin), and the nucleus in control, and *Fam98a*-, *Ndel1*-knocking-down osteoclasts cultured on glass coverslips. Scale bar = 20 µm. (D) and (E) Quantifications of lysosome distribution at the cell periphery and the peri-nuclear regions in immunofluorescence-stained LAMP-2 and cathepsin K (CTSK) in control and *Fam98a*-, *Ndel1*-knocking-down osteoclasts (n = 15) cultured on glass coverslips using Zen 2.0 Blue Profile View software (Zeiss). See figure legend of the supplemental Figure 8B-8C for the detailed methodology. * $p < 0.05$, ** $p < 0.01$, and *** $p < 0.001$ versus *LUC-sh* expressing osteoclasts by one-way ANOVA. Data in (A), (D), and (E) are presented as scatter dot plots. The mean and standard deviation of each group are overlaid onto each column of dots. (F) in vivo and in vitro working models of this study.

Supplemental Tables in word document file

Table 1: µCT analysis of L4 spine

Mouse strain	age	sex	genotype	bone parameters			
				BV/TV (%)	Tb. N (/mm)	Tb. Th (µm)	Tb. Sp (µm)
germline	2-month-old	Male	WT (n=17)	29.17±3.15	5.66±0.23	51.71±3.28	165.49±8.57
			KO (n=17)	40.45±4.78**	7.57±0.50**	55.44±3.64**	119.79±10.44**
		Female	WT (n=11)	27.35±1.91	5.19±0.24	51.55±1.64	183.25±9.56
			KO (n=15)	36.71±2.23**	6.48±0.24**	55.79±2.17**	142.10±7.03**
	5-month-old	Male	WT (n=11)	26.79±1.81	5.21±0.18	50.80±1.72	180.03±7.51
			KO (n=10)	41.35±3.07**	6.99±0.36**	57.03±2.32**	125.89±8.50**
	6-month-old	Female	WT (n=9)	23.76±1.94	4.16±0.21	53.09±2.17	232.42±12.75
			KO (n=9)	38.60±5.60**	5.74±0.59**	60.29±3.64**	161.21±20.43**
conditional	2-month-old	Male	con (n=15)	30.20±2.46	5.97±0.20	50.81±2.31	155.26±6.78
			cKO (n=12)	39.37±3.75**	7.63±0.27**	53.92±3.95	116.37±4.79**
		Female	con (n=14)	27.20±1.87	5.50±0.28	49.32±1.84	172.83±10.40
			cKO (n=14)	37.63±2.04**	6.94±0.31**	53.07±1.91**	130.39±6.98**
	5-month-old	Male	con (n=10)	28.53±3.18	5.26±0.38	51.18±2.90	177.13±18.27
			cKO (n=11)	40.34±3.10**	6.98±0.26**	54.66±2.28**	124.58±5.97**
	6-month-old	Female	con (n=8)	27.43±4.29	4.37±0.44	55.23±3.25	222.00±24.26
			con (n=6)	37.17±5.65**	5.66±0.61$^{\#\#}$	58.90±3.50	162.87±19.82$^{\#\#}$

BV/TV, percentage of trabecular bone volume to tissue volume; Tb. N, trabecular number; Tb. Th, trabecular thickness; Tb.Sp, trabecular separation. **:$p<0.01$ by Student t-test (KO vs WT, Plekhm1; cKO vs con). $^{\#\#}$:$p<0.01$ by Mann-Whitney U statistic test (cKO vs con)

Table 2: µCT analysis of cortical thickness in femur

Mouse strain	age	sex	genotype	Cortical Thickness (mm)
germline	2-month-old	Male	WT (n=17)	0.19±0.012
			KO (n=17)	0.18±0.013
		Female	WT (n=11)	0.18±0.0058
			KO (n=15)	0.17±0.0063**
	5-month-old	Male	WT (n=11)	0.22±0.0048
			KO (n=10)	0.21±0.0067
	6-month-old	Female	WT (n=9)	0.22±0.069
			KO (n=9)	0.22±0.075
conditional	2-month-old	Male	con (n=15)	0.19±0.0080
			cKO (n=12)	0.18±0.017
		Female	con (n=14)	0.17±0.0066
			cKO (n=14)	0.17±0.0074
	5-month-old	Male	con (n=10)	0.22±0.0062
			cKO (n=11)	0.21±0.015*
	6-month-old	Female	con (n=8)	0.23±0.013
			cKO (n=6)	0.22±0.012

*:$p<0.05$, **:$p<0.01$ by student t-test (KO vs WT, cKO vs con)

Table 3: Histomorphometry of the distal femur in 2-month-old male mice

Parameters	Plekhm1;Hprt		Plekhm1;Ctsk	
	WT (n=13)	KO (n=13)	con (n=15)	cKO (n=12)
BV/TV (%)	9.65±2.23	18.75±5.57**	11.96±2.24	21.72±5.13**
Tb. N (/mm)	2.91±0.39	5.05±0.75**	3.43±0.50	5.71±0.93**
Tb. Th (µm)	33.11±6.25	36.59±5.08	34.87±4.23	37.79±5.48
Tb. Sp (µm)	316.98±53.43	165.10±30.44**	262.31±41.38	141.82±33.40**
OV/BV (%)	3.25±1.53	1.66±0.66**	2.79±0.71	1.35±0.40**
O. Th (µm)	2.81±0.30	2.74±0.31	2.95±0.33	3.05±0.30
Ot. N/B. Ar	1096.86±83.09	1268.14±123.00**	1057.50±108.81	1155.57±111.25*

BV/TV, percentage of trabecular bone volume to tissue volume; Tb. N, trabecular number; Tb. Th, trabecular thickness; Tb.Sp, trabecular separation; OV/BV, percentage of osteoid volume to bone volume; O.Th, osteoid thickness; Ot.N/B.Ar, osteocyte number/ bone area. *:$p<0.05$, **:$p<0.01$ student t-test (Plekhm1;Hprt: vs WT, Plekhm1;Ctsk: vs con)

Table 4. PLEKHM1-interacting proteins identified by mass-spectrometry in osteoclasts.

Protein	Accession Number	Molecular Weight	Fold Change	vector spectra	PLEKHM1 spectra
Pleckstrin homology domain-containing family M member 1 OS=Mus musculus GN=Plekhm1 PE=2 SV=1	PKHM1_MOUSE	119 kDa	INF	0	562
Differentially expressed in FDCP 8 OS=Mus musculus GN=Def8 PE=2 SV=1	DEFI8_MOUSE	52 kDa	INF	0	40
Keratin, type I cytoskeletal 40 OS=Mus musculus GN=Krt40 PE=2 SV=1	K1C40_MOUSE	49 kDa	INF	0	22
NADH dehydrogenase [ubiquinone] 1 alpha subcomplex subunit 8 OS=Mus musculus GN=Ndufa8 PE=1 SV=3	NDUA8_MOUSE	20 kDa	INF	0	9
40S ribosomal protein S9 OS=Mus musculus GN=Rps9 PE=2 SV=3	RS9_MOUSE	23 kDa	INF	0	9
Eukaryotic translation initiation factor 3 subunit K OS=Mus musculus GN=Eif3k PE=1 SV=1	EIF3K_MOUSE	25 kDa	INF	0	9
Desmoglein-1-alpha OS=Mus musculus GN=Dsg1a PE=2 SV=2	DSG1A_MOUSE (+1)	115 kDa	INF	0	9
Protein FAM98A OS=Mus musculus GN=Fam98a PE=2 SV=1	FA98A_MOUSE	55 kDa	INF	0	9
Non-histone chromosomal protein HMG-17 OS=Mus musculus GN=Hmgn2 PE=1 SV=2	HMGN2_MOUSE	9 kDa	INF	0	8
Mitogen-activated protein kinase kinase kinase 7 OS=Mus musculus GN=Map3k7 PE=1 SV=1	M3K7_MOUSE	64 kDa	INF	0	8
60S ribosomal protein L6 OS=Mus musculus GN=Rpl6 PE=1 SV=3	RL6_MOUSE	34 kDa	INF	0	7
Protein FAM195A OS=Mus musculus GN=Fam195a PE=1 SV=1	F195A_MOUSE	18 kDa	INF	0	7
Ubiquitin carboxyl-terminal hydrolase 10 OS=Mus musculus GN=Usp10 PE=1 SV=3	UBP10_MOUSE	87 kDa	INF	0	6
Protein regulator of cytokinesis 1 OS=Mus musculus GN=Prc1 PE=2 SV=2	PRC1_MOUSE	70 kDa	INF	0	6
Histone acetyltransferase p300 OS=Mus musculus GN=Ep300 PE=1 SV=1	EP300_MOUSE	264 kDa	INF	0	6
Nuclear cap-binding protein subunit 1 OS=Mus musculus GN=Ncbp1 PE=1 SV=2	NCBP1_MOUSE	92 kDa	INF	0	6
Vesicle-associated membrane protein-associated protein A OS=Mus musculus GN=Vapa PE=1 SV=2	VAPA_MOUSE	28 kDa	INF	0	6
Atherin OS=Mus musculus GN=Samd1 PE=1 SV=1	SAMD1_MOUSE	55 kDa	INF	0	6
Nuclear distribution protein nudE-like 1 OS=Mus musculus GN=Ndel1 PE=1 SV=2	NDEL1_MOUSE	38 kDa	INF	0	6
Probable ubiquitin carboxyl-terminal hydrolase FAF-X OS=Mus musculus GN=Usp9x PE=1 SV=2	USP9X_MOUSE	291 kDa	INF	0	5
Cluster of Cytochrome c, somatic OS=Mus musculus GN=Cycs PE=1 SV=2 (CYC_MOUSE)	CYC_MOUSE	12 kDa	INF	0	5
Zinc finger CCCH domain-containing protein 14 OS=Mus musculus GN=Zc3h14 PE=1 SV=1	ZC3HE_MOUSE	82 kDa	INF	0	5
Helicase with zinc finger domain 2 OS=Mus musculus GN=Helz2 PE=1 SV=1	HELZ2_MOUSE	332 kDa	INF	0	5
RNA-binding protein 47 OS=Mus musculus GN=Rbm47 PE=2 SV=1	RBM47_MOUSE	64 kDa	INF	0	5
Ig kappa chain V-V region MOPC 149 OS=Mus musculus PE=1 SV=1	KV5A4_MOUSE	12 kDa	INF	0	5
DNA dC->dU-editing enzyme APOBEC-3 OS=Mus musculus GN=Apobec3 PE=1 SV=2	ABEC3_MOUSE	51 kDa	INF	0	5

Plakophilin-1 OS=Mus musculus GN=Pkp1 PE=2 SV=1	PKP1_MOUSE	81 kDa	INF	0	5
Leucine-rich repeat-containing protein 7 OS=Mus musculus GN=Lrrc7 PE=1 SV=2	LRRC7_MOUSE	167 kDa	INF	0	5
Four and a half LIM domains protein 3 OS=Mus musculus GN=Fhl3 PE=1 SV=2	FHL3_MOUSE	32 kDa	INF	0	4
Ras-related protein Rap-1b OS=Mus musculus GN=Rap1b PE=2 SV=2	RAP1B_MOUSE	21 kDa	INF	0	4
Eukaryotic translation initiation factor 4E OS=Mus musculus GN=Eif4e PE=1 SV=1	IF4E_MOUSE	25 kDa	INF	0	4
Cation-independent mannose-6-phosphate receptor OS=Mus musculus GN=Igf2r PE=1 SV=1	MPRI_MOUSE	274 kDa	INF	0	4
Phosphatidylserine decarboxylase proenzyme OS=Mus musculus GN=Pisd PE=2 SV=1	PISD_MOUSE	46 kDa	INF	0	4
High affinity immunoglobulin gamma Fc receptor I OS=Mus musculus GN=Fcgr1 PE=1 SV=1	FCGR1_MOUSE	45 kDa	INF	0	4
Serine-rich coiled-coil domain-containing protein 1 OS=Mus musculus GN=Ccser1 PE=2 SV=2	CCSE1_MOUSE	98 kDa	INF	0	4
NADH dehydrogenase [ubiquinone] iron-sulfur protein 5 OS=Mus musculus GN=Ndufs5 PE=1 SV=3	NDUS5_MOUSE	13 kDa	INF	0	4
Protein unc-119 homolog B OS=Mus musculus GN=Unc119b PE=2 SV=1	U119B_MOUSE	28 kDa	INF	0	4
Zinc finger CCCH-type antiviral protein 1 OS=Mus musculus GN=Zc3hav1 PE=1 SV=1	ZCCHV_MOUSE	107 kDa	INF	0	4
Proteasome subunit alpha type-1 OS=Mus musculus GN=Psma1 PE=1 SV=1	PSA1_MOUSE	30 kDa	INF	0	4
Meiosis arrest female protein 1 OS=Mus musculus GN=Marf1 PE=1 SV=3	MARF1_MOUSE	192 kDa	INF	0	4
39S ribosomal protein L28, mitochondrial OS=Mus musculus GN=Mrpl28 PE=2 SV=3	RM28_MOUSE	30 kDa	INF	0	4
14-3-3 protein sigma OS=Mus musculus GN=Sfn PE=1 SV=2	1433S_MOUSE	28 kDa	INF	0	4
TAF6-like RNA polymerase II p300/CBP-associated factor-associated factor 65 kDa subunit 6L OS=Mus musculus GN=Taf6l PE=2 SV=1	TAF6L_MOUSE	67 kDa	INF	0	3
Histone H3.1 OS=Mus musculus GN=Hist1h3a PE=1 SV=2	H31_MOUSE (+3)	15 kDa	INF	0	3
Uncharacterized protein C19orf43 homolog OS=Mus musculus PE=2 SV=1	CS043_MOUSE	18 kDa	INF	0	3
Eukaryotic translation initiation factor 4E transporter OS=Mus musculus GN=Eif4enif1 PE=1 SV=2	4ET_MOUSE	108 kDa	INF	0	3
Charged multivesicular body protein 4b OS=Mus musculus GN=Chmp4b PE=2 SV=2	CHM4B_MOUSE	25 kDa	INF	0	3
Translation machinery-associated protein 7 OS=Mus musculus GN=Tma7 PE=2 SV=1	TMA7_MOUSE	7 kDa	INF	0	3
Signal recognition particle 14 kDa protein OS=Mus musculus GN=Srp14 PE=1 SV=1	SRP14_MOUSE	13 kDa	INF	0	3
Double-stranded RNA-binding protein Staufen homolog 1 OS=Mus musculus GN=Stau1 PE=2 SV=1	STAU1_MOUSE	54 kDa	INF	0	3
CDKN2AIP N-terminal-like protein OS=Mus musculus GN=Cdkn2aipnl PE=2 SV=1	C2AIL_MOUSE	13 kDa	INF	0	3
PCNA-associated factor OS=Mus musculus GN=Paf PE=2 SV=1	PAF15_MOUSE	12 kDa	INF	0	3
39S ribosomal protein L13, mitochondrial OS=Mus musculus GN=Mrpl13 PE=2 SV=1	RM13_MOUSE	21 kDa	INF	0	3

Chromobox protein homolog 3 OS=Mus musculus GN=Cbx3 PE=1 SV=2	CBX3_MOUSE	21 kDa	INF	0	3
CDP-diacylglycerol--inositol 3-phosphatidyltransferase OS=Mus musculus GN=Cdipt PE=1 SV=1	CDIPT_MOUSE	24 kDa	INF	0	3
Small nuclear ribonucleoprotein Sm D2 OS=Mus musculus GN=Snrpd2 PE=1 SV=1	SMD2_MOUSE	14 kDa	INF	0	3
XIAP-associated factor 1 OS=Mus musculus GN=Xaf1 PE=2 SV=3	XAF1_MOUSE	31 kDa	INF	0	3
Mitochondrial fission regulator 1-like OS=Mus musculus GN=Mtfr1l PE=1 SV=1	MFR1L_MOUSE	32 kDa	INF	0	3
60S ribosomal protein L37 OS=Mus musculus GN=Rpl37 PE=2 SV=3	RL37_MOUSE	11 kDa	INF	0	3
Transcription factor Sp1 OS=Mus musculus GN=Sp1 PE=1 SV=2	SP1_MOUSE	81 kDa	INF	0	3
Trinucleotide repeat-containing gene 6A protein OS=Mus musculus GN=Tnrc6a PE=2 SV=1	TNR6A_MOUSE	203 kDa	INF	0	3
DnaJ homolog subfamily C member 15 OS=Mus musculus GN=Dnajc15 PE=1 SV=1	DJC15_MOUSE	16 kDa	INF	0	3
Vesicle-associated membrane protein 8 OS=Mus musculus GN=Vamp8 PE=1 SV=1	VAMP8_MOUSE	11 kDa	INF	0	3
Mitochondrial import inner membrane translocase subunit TIM14 OS=Mus musculus GN=Dnajc19 PE=2 SV=3	TIM14_MOUSE	12 kDa	INF	0	3
Cluster of Microtubule-associated serine/threonine-protein kinase 3 OS=Mus musculus GN=Mast3 PE=1 SV=3 (MAST3_MOUSE)	MAST3_MOUSE	144 kDa	INF	0	3
Microtubule-associated serine/threonine-protein kinase 2 OS=Mus musculus GN=Mast2 PE=1 SV=1	MAST2_MOUSE	191 kDa	INF	0	3
Rho-related GTP-binding protein RhoG OS=Mus musculus GN=Rhog PE=2 SV=1	RHOG_MOUSE	21 kDa	INF	0	3
C-C motif chemokine 9 OS=Mus musculus GN=Ccl9 PE=1 SV=1	CCL9_MOUSE	14 kDa	INF	0	2
28S ribosomal protein S16, mitochondrial OS=Mus musculus GN=Mrps16 PE=2 SV=1	RT16_MOUSE	15 kDa	INF	0	2
Exocyst complex component 4 OS=Mus musculus GN=Exoc4 PE=1 SV=2	EXOC4_MOUSE	111 kDa	INF	0	2
NADH dehydrogenase [ubiquinone] 1 alpha subcomplex subunit 6 OS=Mus musculus GN=Ndufa6 PE=1 SV=1	NDUA6_MOUSE	15 kDa	INF	0	2
Survival motor neuron protein OS=Mus musculus GN=Smn1 PE=1 SV=1	SMN_MOUSE	31 kDa	INF	0	2
2'-5'-oligoadenylate synthase-like protein 1 OS=Mus musculus GN=Oasl1 PE=2 SV=1	OASL1_MOUSE	59 kDa	INF	0	2
AN1-type zinc finger protein 2A OS=Mus musculus GN=Zfand2a PE=2 SV=1	ZFN2A_MOUSE	19 kDa	INF	0	2
Constitutive coactivator of PPAR-gamma-like protein 2 OS=Mus musculus GN=Fam120c PE=2 SV=3	F120C_MOUSE	120 kDa	INF	0	2
Zinc finger protein 608 OS=Mus musculus GN=Znf608 PE=2 SV=1	ZN608_MOUSE	162 kDa	INF	0	2
Transcription elongation factor B polypeptide 3 OS=Mus musculus GN=Tceb3 PE=1 SV=3	ELOA1_MOUSE	87 kDa	INF	0	2
Nucleolar protein 14 OS=Mus musculus GN=Nop14 PE=1 SV=2	NOP14_MOUSE	99 kDa	INF	0	2
Proteasome subunit beta type-6 OS=Mus musculus GN=Psmb6 PE=1 SV=3	PSB6_MOUSE	25 kDa	INF	0	2
28S ribosomal protein S7, mitochondrial OS=Mus musculus GN=Mrps7 PE=2 SV=1	RT07_MOUSE	28 kDa	INF	0	2

Ubiquitin-like modifier-activating enzyme 1 OS=Mus musculus GN=Uba1 PE=1 SV=1	UBA1_MOUSE	118 kDa	INF	0	2
GTP-binding protein Rit1 OS=Mus musculus GN=Rit1 PE=1 SV=1	RIT1_MOUSE	25 kDa	INF	0	2
Ras-related protein Rab-38 OS=Mus musculus GN=Rab38 PE=1 SV=1	RAB38_MOUSE	24 kDa	INF	0	2
Non-specific lipid-transfer protein OS=Mus musculus GN=Scp2 PE=1 SV=3	NLTP_MOUSE	59 kDa	INF	0	2
Mitochondrial import receptor subunit TOM34 OS=Mus musculus GN=Tomm34 PE=2 SV=1	TOM34_MOUSE	34 kDa	INF	0	2
Coiled-coil domain-containing protein 9 OS=Mus musculus GN=Ccdc9 PE=2 SV=1	CCDC9_MOUSE	61 kDa	INF	0	2
Protein SCO2 homolog, mitochondrial OS=Mus musculus GN=Sco2 PE=2 SV=1	SCO2_MOUSE	29 kDa	INF	0	2
ATP synthase subunit delta, mitochondrial OS=Mus musculus GN=Atp5d PE=1 SV=1	ATPD_MOUSE	18 kDa	INF	0	2
A-kinase anchor protein 8 OS=Mus musculus GN=Akap8 PE=1 SV=1	AKAP8_MOUSE	76 kDa	INF	0	2
Disrupted in schizophrenia 1 homolog OS=Mus musculus GN=Disc1 PE=1 SV=2	DISC1_MOUSE	93 kDa	INF	0	2
Elongation factor 1-gamma OS=Mus musculus GN=Eef1g PE=1 SV=3	EF1G_MOUSE	50 kDa	INF	0	2
Importin subunit alpha-4 OS=Mus musculus GN=Kpna3 PE=1 SV=1	IMA4_MOUSE	58 kDa	INF	0	2
LYR motif-containing protein 5 OS=Mus musculus GN=Lyrm5 PE=2 SV=1	LYRM5_MOUSE	10 kDa	INF	0	2
PHD finger-like domain-containing protein 5A OS=Mus musculus GN=Phf5a PE=1 SV=1	PHF5A_MOUSE	12 kDa	INF	0	2
tRNA pseudouridine synthase-like 1 OS=Mus musculus GN=Pusl1 PE=2 SV=1	PUSL1_MOUSE	32 kDa	INF	0	2
Protein S100-A4 OS=Mus musculus GN=S100a4 PE=1 SV=1	S10A4_MOUSE	12 kDa	INF	0	2
Myeloid cell nuclear differentiation antigen-like protein OS=Mus musculus GN=Mndal PE=1 SV=1	MNDAL_MOUSE	61 kDa	INF	0	2
Protein BUD31 homolog OS=Mus musculus GN=Bud31 PE=2 SV=1	BUD31_MOUSE	12 kDa	INF	0	2
C-Myc-binding protein OS=Mus musculus GN=Mycbp PE=2 SV=5	MYCBP_MOUSE	12 kDa	INF	0	2
UPF0468 protein C16orf80 homolog OS=Mus musculus GN=Gtl3 PE=2 SV=1	CP080_MOUSE	23 kDa	INF	0	2
Calcineurin-like phosphoesterase domain-containing protein 1 OS=Mus musculus GN=Cpped1 PE=2 SV=1	CPPED_MOUSE	35 kDa	INF	0	2
Insulin-like growth factor 2 mRNA-binding protein 2 OS=Mus musculus GN=Igf2bp2 PE=1 SV=1	IF2B2_MOUSE	66 kDa	INF	0	2
NADH dehydrogenase [ubiquinone] iron-sulfur protein 6, mitochondrial OS=Mus musculus GN=Ndufs6 PE=1 SV=2	NDUS6_MOUSE	13 kDa	INF	0	2
Peptidyl-prolyl cis-trans isomerase-like 1 OS=Mus musculus GN=Ppil1 PE=2 SV=1	PPIL1_MOUSE	18 kDa	INF	0	2
28S ribosomal protein S23, mitochondrial OS=Mus musculus GN=Mrps23 PE=2 SV=1	RT23_MOUSE	20 kDa	INF	0	2
DNA polymerase sigma OS=Mus musculus GN=Papd7 PE=2 SV=2	PAPD7_MOUSE	60 kDa	INF	0	2
Clathrin light chain A OS=Mus musculus GN=Clta PE=2 SV=2	CLCA_MOUSE	26 kDa	INF	0	2

TRAF-type zinc finger domain-containing protein 1 OS=Mus musculus GN=Trafd1 PE=1 SV=1	TRAD1_MOUSE	64 kDa	INF	0	2
Calpain-2 catalytic subunit OS=Mus musculus GN=Capn2 PE=2 SV=4	CAN2_MOUSE	80 kDa	INF	0	2
cAMP-dependent protein kinase type I-alpha regulatory subunit OS=Mus musculus GN=Prkar1a PE=1 SV=3	KAP0_MOUSE	43 kDa	INF	0	2
Protein CASC3 OS=Mus musculus GN=Casc3 PE=1 SV=3	CASC3_MOUSE	76 kDa	INF	0	2
Delphilin OS=Mus musculus GN=Grid2ip PE=1 SV=1	GRD2I_MOUSE	132 kDa	INF	0	2
CDGSH iron-sulfur domain-containing protein 1 OS=Mus musculus GN=Cisd1 PE=1 SV=1	CISD1_MOUSE	12 kDa	INF	0	2
Serine/threonine-protein kinase TAO1 OS=Mus musculus GN=Taok1 PE=1 SV=1	TAOK1_MOUSE	116 kDa	INF	0	2
Putative ATP-dependent RNA helicase DHX30 OS=Mus musculus GN=Dhx30 PE=2 SV=1	DHX30_MOUSE	137 kDa	18	1	18
Probable JmjC domain-containing histone demethylation protein 2C OS=Mus musculus GN=Jmjd1c PE=1 SV=3	JHD2C_MOUSE	261 kDa	17	3	50
G2 and S phase-expressed protein 1 OS=Mus musculus GN=Gtse1 PE=1 SV=2	GTSE1_MOUSE	79 kDa	16	1	16
Tetratricopeptide repeat protein 28 OS=Mus musculus GN=Ttc28 PE=2 SV=3	TTC28_MOUSE	267 kDa	14	1	14
Tudor domain-containing protein 3 OS=Mus musculus GN=Tdrd3 PE=1 SV=4	TDRD3_MOUSE	82 kDa	13	1	13
40S ribosomal protein S21 OS=Mus musculus GN=Rps21 PE=2 SV=1	RS21_MOUSE	9 kDa	11	1	11
Eukaryotic translation initiation factor 3 subunit M OS=Mus musculus GN=Eif3m PE=2 SV=1	EIF3M_MOUSE	43 kDa	10	1	10
39S ribosomal protein L4, mitochondrial OS=Mus musculus GN=Mrpl4 PE=2 SV=1	RM04_MOUSE	33 kDa	10	1	10
Protein TALPID3 OS=Mus musculus GN=Talpid3 PE=2 SV=1	TALD3_MOUSE	167 kDa	10	1	10
Cancer-related nucleoside-triphosphatase homolog OS=Mus musculus GN=Ntpcr PE=2 SV=1	NTPCR_MOUSE	21 kDa	9	1	9
TGF-beta-activated kinase 1 and MAP3K7-binding protein 1 OS=Mus musculus GN=Tab1 PE=1 SV=2	TAB1_MOUSE	55 kDa	9	1	9
Polypyrimidine tract-binding protein 1 OS=Mus musculus GN=Ptbp1 PE=1 SV=2	PTBP1_MOUSE	56 kDa	9	1	9
Fragile X mental retardation protein 1 homolog OS=Mus musculus GN=Fmr1 PE=1 SV=1	FMR1_MOUSE	69 kDa	8.4	7	47
60S ribosomal protein L26 OS=Mus musculus GN=Rpl26 PE=2 SV=1	RL26_MOUSE	17 kDa	8	2	16
Protein LYRIC OS=Mus musculus GN=Mtdh PE=1 SV=1	LYRIC_MOUSE	64 kDa	8	1	8
Serine/threonine-protein kinase DCLK1 OS=Mus musculus GN=Dclk1 PE=1 SV=1	DCLK1_MOUSE	84 kDa	8	1	8
Putative helicase MOV-10 OS=Mus musculus GN=Mov10 PE=1 SV=2	MOV10_MOUSE	114 kDa	7.3	3	22
Kinesin-like protein KIFC1 OS=Mus musculus GN=Kifc1 PE=1 SV=2	KIFC1_MOUSE	74 kDa	7.3	3	22
Cytochrome c1, heme protein, mitochondrial OS=Mus musculus GN=Cyc1 PE=1 SV=1	CY1_MOUSE	35 kDa	7	1	7
Zinc finger protein 703 OS=Mus musculus GN=Znf703 PE=1 SV=1	ZN703_MOUSE	59 kDa	7	1	7

YTH domain family protein 3 OS=Mus musculus GN=Ythdf3 PE=1 SV=2	YTHD3_MOUSE	64 kDa	7	1	7
C2 domain-containing protein 2-like OS=Mus musculus GN=C2cd2l PE=1 SV=3	C2C2L_MOUSE	76 kDa	6.7	6	20
La-related protein 1 OS=Mus musculus GN=Larp1 PE=1 SV=2	LARP1_MOUSE	121 kDa	6.5	4	26
Lysine--tRNA ligase OS=Mus musculus GN=Kars PE=1 SV=1	SYK_MOUSE	68 kDa	6.5	2	13
Desmoplakin OS=Mus musculus GN=Dsp PE=1 SV=1	DESP_MOUSE	333 kDa	6.4	14	89
EGF-like repeat and discoidin I-like domain-containing protein 3 OS=Mus musculus GN=Edil3 PE=1 SV=2	EDIL3_MOUSE	54 kDa	6.2	4	25
Protein PRRC2C OS=Mus musculus GN=Prrc2c PE=1 SV=3	PRC2C_MOUSE	311 kDa	6.1	36	218
Eukaryotic translation initiation factor 3 subunit H OS=Mus musculus GN=Eif3h PE=1 SV=1	EIF3H_MOUSE	40 kDa	6	3	18
Targeting protein for Xklp2 OS=Mus musculus GN=Tpx2 PE=1 SV=1	TPX2_MOUSE	86 kDa	6	1	6
39S ribosomal protein L32, mitochondrial OS=Mus musculus GN=Mrpl32 PE=2 SV=1	RM32_MOUSE	22 kDa	6	1	6
Calcium-binding mitochondrial carrier protein Aralar1 OS=Mus musculus GN=Slc25a12 PE=1 SV=1	CMC1_MOUSE	75 kDa	6	1	6
AT-rich interactive domain-containing protein 5B OS=Mus musculus GN=Arid5b PE=1 SV=3	ARI5B_MOUSE	132 kDa	6	1	6
Muscleblind-like protein 2 OS=Mus musculus GN=Mbnl2 PE=2 SV=2	MBNL2_MOUSE	40 kDa	6	1	6
39S ribosomal protein L16, mitochondrial OS=Mus musculus GN=Mrpl16 PE=2 SV=1	RM16_MOUSE	29 kDa	6	1	6
Macrophage scavenger receptor types I and II OS=Mus musculus GN=Msr1 PE=1 SV=3	MSRE_MOUSE	50 kDa	6	1	6
Fragile X mental retardation syndrome-related protein 1 OS=Mus musculus GN=Fxr1 PE=1 SV=2	FXR1_MOUSE	76 kDa	5.9	21	125
Eukaryotic translation initiation factor 3 subunit I OS=Mus musculus GN=Eif3i PE=1 SV=1	EIF3I_MOUSE	36 kDa	5.7	3	17
Heterogeneous nuclear ribonucleoprotein Q OS=Mus musculus GN=Syncrip PE=1 SV=2	HNRPQ_MOUSE	70 kDa	5.6	7	39
Regulator of nonsense transcripts 1 OS=Mus musculus GN=Upf1 PE=1 SV=2	RENT1_MOUSE	124 kDa	5.3	18	96
Eukaryotic translation initiation factor 3 subunit C OS=Mus musculus GN=Eif3c PE=1 SV=1	EIF3C_MOUSE	106 kDa	5.3	7	37
Eukaryotic translation initiation factor 3 subunit A OS=Mus musculus GN=Eif3a PE=1 SV=5	EIF3A_MOUSE	162 kDa	5.2	13	68
Guanine nucleotide-binding protein subunit beta-2-like 1 OS=Mus musculus GN=Gnb2l1 PE=1 SV=3	GBLP_MOUSE	35 kDa	5.2	4	21
Serum albumin OS=Mus musculus GN=Alb PE=1 SV=3	ALBU_MOUSE	69 kDa	5	3	15
40S ribosomal protein S15 OS=Mus musculus GN=Rps15 PE=2 SV=2	RS15_MOUSE	17 kDa	5	2	10
D-beta-hydroxybutyrate dehydrogenase, mitochondrial OS=Mus musculus GN=Bdh1 PE=1 SV=2	BDH_MOUSE	38 kDa	5	2	10
Transcriptional repressor NF-X1 OS=Mus musculus GN=Nfx1 PE=2 SV=1	NFX1_MOUSE	124 kDa	5	2	10
NADH dehydrogenase [ubiquinone] iron-sulfur protein 7, mitochondrial OS=Mus musculus GN=Ndufs7 PE=1 SV=1	NDUS7_MOUSE	25 kDa	5	1	5
Calcium-independent phospholipase A2-gamma OS=Mus musculus GN=Pnpla8 PE=2 SV=1	PLPL8_MOUSE	87 kDa	5	1	5

Leucine--tRNA ligase, cytoplasmic OS=Mus musculus GN=Lars PE=2 SV=2	SYLC_MOUSE	134 kDa	5	1	5
Transgelin-2 OS=Mus musculus GN=Tagln2 PE=1 SV=4	TAGL2_MOUSE	22 kDa	5	1	5
Cluster of GTPase HRas OS=Mus musculus GN=Hras1 PE=1 SV=2 (RASH_MOUSE)	RASH_MOUSE	21 kDa	5	1	5
Protein disulfide-isomerase A3 OS=Mus musculus GN=Pdia3 PE=1 SV=2	PDIA3_MOUSE	57 kDa	5	1	5
RAS protein activator like-3 OS=Mus musculus GN=Rasal3 PE=2 SV=1	RASL3_MOUSE	115 kDa	5	1	5
Syntaxin-7 OS=Mus musculus GN=Stx7 PE=1 SV=3	STX7_MOUSE	30 kDa	5	1	5
Tristetraprolin OS=Mus musculus GN=Zfp36 PE=1 SV=1	TTP_MOUSE	34 kDa	5	1	5
Serine/threonine-protein kinase A-Raf OS=Mus musculus GN=Araf PE=2 SV=2	ARAF_MOUSE	68 kDa	5	1	5
Torsin-4A OS=Mus musculus GN=Tor4a PE=2 SV=1	TOR4A_MOUSE	48 kDa	5	1	5
Cluster of Protein argonaute-2 OS=Mus musculus GN=Ago2 PE=1 SV=3 (AGO2_MOUSE)	AGO2_MOUSE [3]	97 kDa	4.8	5	24
Eukaryotic translation initiation factor 4B OS=Mus musculus GN=Eif4b PE=1 SV=1	IF4B_MOUSE	69 kDa	4.8	4	19
5'-3' exoribonuclease 2 OS=Mus musculus GN=Xrn2 PE=1 SV=1	XRN2_MOUSE	109 kDa	4.7	3	14
40S ribosomal protein S6 OS=Mus musculus GN=Rps6 PE=1 SV=1	RS6_MOUSE	29 kDa	4.7	3	14
NADH dehydrogenase [ubiquinone] 1 beta subcomplex subunit 4 OS=Mus musculus GN=Ndufb4 PE=1 SV=3	NDUB4_MOUSE	15 kDa	4.7	3	14
Cluster of Neuron navigator 1 OS=Mus musculus GN=Nav1 PE=1 SV=2 (NAV1_MOUSE)	NAV1_MOUSE	202 kDa	4.5	14	63
ELAV-like protein 1 OS=Mus musculus GN=Elavl1 PE=1 SV=2	ELAV1_MOUSE	36 kDa	4.5	4	18
Heterogeneous nuclear ribonucleoprotein A3 OS=Mus musculus GN=Hnrnpa3 PE=1 SV=1	ROA3_MOUSE	40 kDa	4.5	2	9
ATP-dependent RNA helicase Dhx29 OS=Mus musculus GN=Dhx29 PE=2 SV=1	DHX29_MOUSE	154 kDa	4.5	2	9
Ras-related C3 botulinum toxin substrate 2 OS=Mus musculus GN=Rac2 PE=2 SV=1	RAC2_MOUSE	21 kDa	4.5	2	9
Casein kinase I isoform alpha OS=Mus musculus GN=Csnk1a1 PE=2 SV=2	KC1A_MOUSE	39 kDa	4.5	2	9
Eukaryotic translation initiation factor 4 gamma 2 OS=Mus musculus GN=Eif4g2 PE=1 SV=2	IF4G2_MOUSE	102 kDa	4.3	3	13
Protein FRG1 OS=Mus musculus GN=Frg1 PE=1 SV=2	FRG1_MOUSE	29 kDa	4.3	3	13
Transmembrane and coiled-coil domains protein 3 OS=Mus musculus GN=Tmcc3 PE=1 SV=2	TMCC3_MOUSE	54 kDa	4.3	3	13
Nuclear fragile X mental retardation-interacting protein 2 OS=Mus musculus GN=Nufip2 PE=1 SV=1	NUFP2_MOUSE	76 kDa	4.2	8	34
Protein PRRC2A OS=Mus musculus GN=Prrc2a PE=1 SV=1	PRC2A_MOUSE	229 kDa	4.1	19	77
Polyadenylate-binding protein 1 OS=Mus musculus GN=Pabpc1 PE=1 SV=2	PABP1_MOUSE	71 kDa	4	37	149
40S ribosomal protein S17 OS=Mus musculus GN=Rps17 PE=1 SV=2	RS17_MOUSE	16 kDa	4	9	36
40S ribosomal protein S26 OS=Mus musculus GN=Rps26 PE=2 SV=3	RS26_MOUSE	13 kDa	4	5	20
Nuclear distribution protein nudE homolog 1 OS=Mus musculus GN=Nde1 PE=1 SV=1	NDE1_MOUSE	39 kDa	4	4	16

LIM domain-containing protein 2 OS=Mus musculus GN=Limd2 PE=2 SV=1	LIMD2_MOUSE	14 kDa	4	3	8
Ig kappa chain V19-17 OS=Mus musculus GN=Igk-V19-17 PE=1 SV=1	KV5A1_MOUSE	16 kDa	4	3	8
Transcription factor Sp2 OS=Mus musculus GN=Sp2 PE=2 SV=2	SP2_MOUSE	65 kDa	4	2	8
Putative RNA-binding protein 3 OS=Mus musculus GN=Rbm3 PE=2 SV=1	RBM3_MOUSE	17 kDa	4	2	8
Ankyrin repeat domain-containing protein 17 OS=Mus musculus GN=Ankrd17 PE=1 SV=2	ANR17_MOUSE	274 kDa	4	2	8
Heterogeneous nuclear ribonucleoprotein H2 OS=Mus musculus GN=Hnrnph2 PE=2 SV=1	HNRH2_MOUSE	49 kDa	4	2	8
Protein FAM110A OS=Mus musculus GN=Fam110a PE=2 SV=2	F110A_MOUSE	32 kDa	4	1	5
ADP-ribosylation factor-like protein 8B OS=Mus musculus GN=Arl8b PE=2 SV=1	ARL8B_MOUSE	22 kDa	4	1	4
Serine/arginine-rich splicing factor 3 OS=Mus musculus GN=Srsf3 PE=1 SV=1	SRSF3_MOUSE	19 kDa	4	1	4
OTU domain-containing protein 4 OS=Mus musculus GN=Otud4 PE=1 SV=1	OTUD4_MOUSE	123 kDa	4	1	4
Cluster of Far upstream element-binding protein 2 OS=Mus musculus GN=Khsrp PE=1 SV=2 (FUBP2_MOUSE)	FUBP2_MOUSE [2]	77 kDa	4	1	4
Active regulator of SIRT1 OS=Mus musculus GN=Rps19bp1 PE=1 SV=1	AROS_MOUSE	16 kDa	4	1	4
Guanine nucleotide-binding protein-like 3-like protein OS=Mus musculus GN=Gnl3l PE=1 SV=1	GNL3L_MOUSE	65 kDa	4	1	4
Histone H4 OS=Mus musculus GN=Hist1h4a PE=1 SV=2	H4_MOUSE	11 kDa	4	1	4
Leukocyte receptor cluster member 1 homolog OS=Mus musculus GN=Leng1 PE=2 SV=1	LENG1_MOUSE	30 kDa	4	1	4
Complement C1q subcomponent subunit A OS=Mus musculus GN=C1qa PE=1 SV=2	C1QA_MOUSE	26 kDa	4	1	4
Casein kinase I isoform delta OS=Mus musculus GN=Csnk1d PE=1 SV=2	KC1D_MOUSE	47 kDa	4	1	4
Calnexin OS=Mus musculus GN=Canx PE=1 SV=1	CALX_MOUSE	67 kDa	4	1	4
Mitochondrial import inner membrane translocase subunit TIM16 OS=Mus musculus GN=Pam16 PE=2 SV=1	TIM16_MOUSE	14 kDa	4	1	4
FERM domain-containing protein 4A OS=Mus musculus GN=Frmd4a PE=1 SV=2	FRM4A_MOUSE	114 kDa	4	1	4
Junction plakoglobin OS=Mus musculus GN=Jup PE=1 SV=3	PLAK_MOUSE	82 kDa	3.9	16	63
DNA replication factor Cdt1 OS=Mus musculus GN=Cdt1 PE=1 SV=1	CDT1_MOUSE	62 kDa	3.8	4	15
Eukaryotic translation initiation factor 3 subunit D OS=Mus musculus GN=Eif3d PE=1 SV=2	EIF3D_MOUSE	64 kDa	3.7	7	26
Cytochrome c oxidase subunit 6C OS=Mus musculus GN=Cox6c PE=1 SV=3	COX6C_MOUSE	8 kDa	3.7	3	11
Ribosomal RNA processing protein 1 homolog B OS=Mus musculus GN=Rrp1b PE=2 SV=2	RRP1B_MOUSE	81 kDa	3.7	3	11
Fragile X mental retardation syndrome-related protein 2 OS=Mus musculus GN=Fxr2 PE=1 SV=1	FXR2_MOUSE	74 kDa	3.6	16	53
40S ribosomal protein S30 OS=Mus musculus GN=Fau PE=3 SV=1	RS30_MOUSE	7 kDa	3.5	4	14

40S ribosomal protein S2 OS=Mus musculus GN=Rps2 PE=2 SV=3	RS2_MOUSE	31 kDa	3.5	4	14
T-complex protein 1 subunit theta OS=Mus musculus GN=Cct8 PE=1 SV=3	TCPQ_MOUSE	60 kDa	3.5	4	14
60S ribosomal protein L17 OS=Mus musculus GN=Rpl17 PE=2 SV=3	RL17_MOUSE	21 kDa	3.5	2	7
Phosphate carrier protein, mitochondrial OS=Mus musculus GN=Slc25a3 PE=1 SV=1	MPCP_MOUSE	40 kDa	3.5	2	7
Peptidyl-prolyl cis-trans isomerase B OS=Mus musculus GN=Ppib PE=2 SV=2	PPIB_MOUSE	24 kDa	3.5	2	7
Rho GTPase-activating protein 22 OS=Mus musculus GN=Arhgap22 PE=1 SV=2	RHG22_MOUSE	78 kDa	3.5	2	7
Vinexin OS=Mus musculus GN=Sorbs3 PE=1 SV=1	VINEX_MOUSE	82 kDa	3.5	2	7
40S ribosomal protein S29 OS=Mus musculus GN=Rps29 PE=2 SV=2	RS29_MOUSE	7 kDa	3.5	2	7
Mitochondrial 2-oxoglutarate/malate carrier protein OS=Mus musculus GN=Slc25a11 PE=1 SV=3	M2OM_MOUSE	34 kDa	3.5	2	7
Tyrosine-protein phosphatase non-receptor type 12 OS=Mus musculus GN=Ptpn12 PE=1 SV=3	PTN12_MOUSE	87 kDa	3.5	2	7
60S ribosomal protein L27a OS=Mus musculus GN=Rpl27a PE=2 SV=5	RL27A_MOUSE	17 kDa	3.5	2	7
Dehydrogenase/reductase SDR family member 7B OS=Mus musculus GN=Dhrs7b PE=2 SV=1	DRS7B_MOUSE	35 kDa	3.5	2	7
ETS domain-containing transcription factor ERF OS=Mus musculus GN=Erf PE=2 SV=1	ERF_MOUSE	59 kDa	3.5	2	7
40S ribosomal protein S18 OS=Mus musculus GN=Rps18 PE=1 SV=3	RS18_MOUSE	18 kDa	3.4	8	27
ATP synthase subunit gamma, mitochondrial OS=Mus musculus GN=Atp5c1 PE=1 SV=1	ATPG_MOUSE	33 kDa	3.3	13	43
40S ribosomal protein S5 OS=Mus musculus GN=Rps5 PE=2 SV=3	RS5_MOUSE	23 kDa	3.3	7	23
Eukaryotic translation initiation factor 3 subunit G OS=Mus musculus GN=Eif3g PE=1 SV=2	EIF3G_MOUSE	36 kDa	3.3	3	10
40S ribosomal protein S10 OS=Mus musculus GN=Rps10 PE=1 SV=1	RS10_MOUSE	19 kDa	3.2	20	66
Ataxin-2-like protein OS=Mus musculus GN=Atxn2l PE=1 SV=1	ATX2L_MOUSE	111 kDa	3.2	9	29
40S ribosomal protein S13 OS=Mus musculus GN=Rps13 PE=2 SV=2	RS13_MOUSE	17 kDa	3.2	5	16
60S ribosomal protein L22-like 1 OS=Mus musculus GN=Rpl22l1 PE=1 SV=1	RL22L_MOUSE	14 kDa	3.2	5	16
Y-box-binding protein 3 OS=Mus musculus GN=Ybx3 PE=1 SV=2	YBOX3_MOUSE	39 kDa	3.1	10	35
Eukaryotic translation initiation factor 4 gamma 1 OS=Mus musculus GN=Eif4g1 PE=1 SV=1	IF4G1_MOUSE	176 kDa	3.1	8	25
Ataxin-2 OS=Mus musculus GN=Atxn2 PE=1 SV=1	ATX2_MOUSE	136 kDa	3	23	69
Nuclease-sensitive element-binding protein 1 OS=Mus musculus GN=Ybx1 PE=1 SV=3	YBOX1_MOUSE	36 kDa	3	23	68
Protein LAP2 OS=Mus musculus GN=Erbb2ip PE=1 SV=3	LAP2_MOUSE	157 kDa	3	15	45
Non-POU domain-containing octamer-binding protein OS=Mus musculus GN=Nono PE=1 SV=3	NONO_MOUSE	55 kDa	3	9	25
Cluster of Serine/threonine-protein kinase WNK1 OS=Mus musculus GN=Wnk1 PE=1 SV=2 (WNK1_MOUSE)	WNK1_MOUSE	251 kDa	3	7	18

Protein SPT2 homolog OS=Mus musculus GN=Spty2d1 PE=2 SV=1	SPT2_MOUSE	75 kDa	3	6	18
La-related protein 4 OS=Mus musculus GN=Larp4 PE=2 SV=2	LARP4_MOUSE	80 kDa	3	6	18
RNA-binding motif protein, X chromosome OS=Mus musculus GN=Rbmx PE=1 SV=1	RBMX_MOUSE (+1)	42 kDa	3	6	18
Eukaryotic translation initiation factor 4 gamma 3 OS=Mus musculus GN=Eif4g3 PE=1 SV=2	IF4G3_MOUSE	175 kDa	3	4	12
5'-3' exoribonuclease 1 OS=Mus musculus GN=Xrn1 PE=1 SV=1	XRN1_MOUSE	194 kDa	3	3	9
Probable pleckstrin homology domain-containing family N member 1 OS=Mus musculus GN=Plekhn1 PE=1 SV=1	PKHN1_MOUSE	39 kDa	3	3	9
Vasculin-like protein 1 OS=Mus musculus GN=Gpbp1l1 PE=1 SV=1	GPBL1_MOUSE	52 kDa	3	2	6
Peptidyl-tRNA hydrolase ICT1, mitochondrial OS=Mus musculus GN=Ict1 PE=1 SV=1	ICT1_MOUSE	23 kDa	3	2	6
Myelin-associated neurite-outgrowth inhibitor OS=Mus musculus GN=Fam168b PE=1 SV=1	F168B_MOUSE	20 kDa	3	2	6
CAP-Gly domain-containing linker protein 2 OS=Mus musculus GN=Clip2 PE=1 SV=2	CLIP2_MOUSE	116 kDa	3	2	6
NADH dehydrogenase (ubiquinone) complex I, assembly factor 6 OS=Mus musculus GN=Ndufaf6 PE=1 SV=1	NDUF6_MOUSE	38 kDa	3	2	6
Platelet-derived growth factor subunit B OS=Mus musculus GN=Pdgfb PE=2 SV=1	PDGFB_MOUSE	27 kDa	3	2	6
Protein transport protein Sec61 subunit beta OS=Mus musculus GN=Sec61b PE=1 SV=3	SC61B_MOUSE	10 kDa	3	2	6
60S ribosomal protein L18a OS=Mus musculus GN=Rpl18a PE=2 SV=1	RL18A_MOUSE	21 kDa	3	1	4
Interferon regulatory factor 2-binding protein 2 OS=Mus musculus GN=Irf2bp2 PE=1 SV=1	I2BP2_MOUSE	59 kDa	3	1	3
39S ribosomal protein L43, mitochondrial OS=Mus musculus GN=Mrpl43 PE=2 SV=1	RM43_MOUSE	20 kDa	3	1	3
Protein TANC2 OS=Mus musculus GN=Tanc2 PE=1 SV=1	TANC2_MOUSE	220 kDa	3	1	3
60S ribosomal protein L13 OS=Mus musculus GN=Rpl13 PE=2 SV=3	RL13_MOUSE	24 kDa	3	1	3
ATP-dependent RNA helicase A OS=Mus musculus GN=Dhx9 PE=1 SV=2	DHX9_MOUSE	149 kDa	3	1	3
Protein FAM65A OS=Mus musculus GN=Fam65a PE=1 SV=2	FA65A_MOUSE	132 kDa	3	1	3
E3 ubiquitin/ISG15 ligase TRIM25 OS=Mus musculus GN=Trim25 PE=1 SV=2	TRI25_MOUSE	72 kDa	3	1	3
Profilin-1 OS=Mus musculus GN=Pfn1 PE=1 SV=2	PROF1_MOUSE	15 kDa	3	1	3
26S proteasome non-ATPase regulatory subunit 3 OS=Mus musculus GN=Psmd3 PE=1 SV=3	PSMD3_MOUSE	61 kDa	3	1	3
NEDD4-like E3 ubiquitin-protein ligase WWP2 OS=Mus musculus GN=Wwp2 PE=1 SV=1	WWP2_MOUSE	99 kDa	3	1	3
Coatomer subunit gamma-1 OS=Mus musculus GN=Copg1 PE=2 SV=1	COPG1_MOUSE	98 kDa	3	1	3
Protein FAM117B OS=Mus musculus GN=Fam117b PE=1 SV=1	F117B_MOUSE	61 kDa	3	1	3
S-formylglutathione hydrolase OS=Mus musculus GN=Esd PE=2 SV=1	ESTD_MOUSE	31 kDa	3	1	3

28S ribosomal protein S33, mitochondrial OS=Mus musculus GN=Mrps33 PE=2 SV=1	RT33_MOUSE	12 kDa	3	1	3
Aminoacyl tRNA synthase complex-interacting multifunctional protein 1 OS=Mus musculus GN=Aimp1 PE=1 SV=2	AIMP1_MOUSE	34 kDa	3	1	3
E3 ubiquitin-protein ligase TRIM56 OS=Mus musculus GN=Trim56 PE=1 SV=1	TRI56_MOUSE	80 kDa	3	1	3
39S ribosomal protein L50, mitochondrial OS=Mus musculus GN=Mrpl50 PE=2 SV=2	RM50_MOUSE	18 kDa	3	1	3
Constitutive coactivator of PPAR-gamma-like protein 1 OS=Mus musculus GN=FAM120A PE=1 SV=2	F120A_MOUSE	122 kDa	2.9	34	100
Neuronal tyrosine-phosphorylated phosphoinositide-3-kinase adapter 2 OS=Mus musculus GN=Nyap2 PE=1 SV=1	NYAP2_MOUSE	74 kDa	2.9	16	47
Serine/threonine-protein phosphatase PGAM5, mitochondrial OS=Mus musculus GN=Pgam5 PE=2 SV=1	PGAM5_MOUSE	32 kDa	2.9	12	35
40S ribosomal protein S8 OS=Mus musculus GN=Rps8 PE=2 SV=2	RS8_MOUSE	24 kDa	2.9	7	20
Heterogeneous nuclear ribonucleoproteins A2/B1 OS=Mus musculus GN=Hnrnpa2b1 PE=1 SV=2	ROA2_MOUSE	37 kDa	2.8	9	25
Protein FAM83G OS=Mus musculus GN=Fam83g PE=2 SV=1	FA83G_MOUSE	90 kDa	2.8	8	22
28S ribosomal protein S12, mitochondrial OS=Mus musculus GN=Mrps12 PE=2 SV=1	RT12_MOUSE	15 kDa	2.8	6	17
14-3-3 protein epsilon OS=Mus musculus GN=Ywhae PE=1 SV=1	1433E_MOUSE	29 kDa	2.8	6	17
Gem-associated protein 5 OS=Mus musculus GN=Gemin5 PE=2 SV=2	GEMI5_MOUSE	167 kDa	2.8	5	14
U6 snRNA-associated Sm-like protein LSm4 OS=Mus musculus GN=Lsm4 PE=2 SV=1	LSM4_MOUSE	15 kDa	2.8	4	11
PTB-containing, cubilin and LRP1-interacting protein OS=Mus musculus GN=Pid1 PE=1 SV=2	PCLI1_MOUSE	25 kDa	2.8	4	11
Cluster of IQ motif and SEC7 domain-containing protein 1 OS=Mus musculus GN=Iqsec1 PE=1 SV=2 (IQEC1_MOUSE)	IQEC1_MOUSE	108 kDa	2.7	15	40
40S ribosomal protein S16 OS=Mus musculus GN=Rps16 PE=2 SV=4	RS16_MOUSE	16 kDa	2.7	13	35
CREB-regulated transcription coactivator 2 OS=Mus musculus GN=Crtc2 PE=1 SV=2	CRTC2_MOUSE	73 kDa	2.7	12	32
CDGSH iron-sulfur domain-containing protein 3, mitochondrial OS=Mus musculus GN=Cisd3 PE=1 SV=1	CISD3_MOUSE	16 kDa	2.7	6	16
ATP synthase subunit e, mitochondrial OS=Mus musculus GN=Atp5i PE=1 SV=2	ATP5I_MOUSE	8 kDa	2.7	3	8
Single-stranded DNA-binding protein, mitochondrial OS=Mus musculus GN=Ssbp1 PE=2 SV=1	SSBP_MOUSE	17 kDa	2.7	3	8
Ras GTPase-activating protein-binding protein 1 OS=Mus musculus GN=G3bp1 PE=1 SV=1	G3BP1_MOUSE	52 kDa	2.6	41	107
40S ribosomal protein S3a OS=Mus musculus GN=Rps3a PE=1 SV=3	RS3A_MOUSE	30 kDa	2.6	30	78
RNA-binding protein 33 OS=Mus musculus GN=Rbm33 PE=1 SV=2	RBM33_MOUSE	137 kDa	2.6	27	70
60S ribosomal protein L23a OS=Mus musculus GN=Rpl23a PE=1 SV=1	RL23A_MOUSE	18 kDa	2.6	9	23
60 kDa heat shock protein, mitochondrial OS=Mus musculus GN=Hspd1 PE=1 SV=1	CH60_MOUSE	61 kDa	2.6	5	13

Serine/arginine-rich splicing factor 1 OS=Mus musculus GN=Srsf1 PE=1 SV=3	SRSF1_MOUSE	28 kDa	2.6	5	13
Eukaryotic translation initiation factor 3 subunit B OS=Mus musculus GN=Eif3b PE=1 SV=1	EIF3B_MOUSE	91 kDa	2.5	13	33
ETS translocation variant 3 OS=Mus musculus GN=Etv3 PE=2 SV=2	ETV3_MOUSE	57 kDa	2.5	6	15
60S ribosomal protein L31 OS=Mus musculus GN=Rpl31 PE=2 SV=1	RL31_MOUSE	14 kDa	2.5	4	10
Adenomatous polyposis coli protein OS=Mus musculus GN=Apc PE=1 SV=1	APC_MOUSE	311 kDa	2.5	4	10
Rho GTPase-activating protein 31 OS=Mus musculus GN=Arhgap31 PE=1 SV=1	RHG31_MOUSE	155 kDa	2.5	4	10
Rab11 family-interacting protein 5 OS=Mus musculus GN=Rab11fip5 PE=1 SV=2	RFIP5_MOUSE	70 kDa	2.5	2	5
UNC119-binding protein C5orf30 homolog OS=Mus musculus GN=D1Ertd622e PE=2 SV=1	CE030_MOUSE	23 kDa	2.5	2	5
UPF0568 protein C14orf166 homolog OS=Mus musculus PE=2 SV=1	CN166_MOUSE	28 kDa	2.5	2	5
Small nuclear ribonucleoprotein-associated protein B OS=Mus musculus GN=Snrpb PE=1 SV=1	RSMB_MOUSE (+1)	24 kDa	2.5	2	5
60S ribosomal protein L8 OS=Mus musculus GN=Rpl8 PE=2 SV=2	RL8_MOUSE	28 kDa	2.5	2	5
Serpin B6 OS=Mus musculus GN=Serpinb6 PE=2 SV=1	SPB6_MOUSE	43 kDa	2.5	2	5
Ig kappa chain V region Mem5 (Fragment) OS=Mus musculus PE=1 SV=1	KVM5_MOUSE	13 kDa	2.5	2	5
Protein LSM14 homolog A OS=Mus musculus GN=Lsm14a PE=1 SV=1	LS14A_MOUSE	51 kDa	2.4	20	48
Ubiquitin-associated protein 2-like OS=Mus musculus GN=Ubap2l PE=1 SV=1	UBP2L_MOUSE	117 kDa	2.4	13	31
Small nuclear ribonucleoprotein Sm D3 OS=Mus musculus GN=Snrpd3 PE=1 SV=1	SMD3_MOUSE	14 kDa	2.4	8	19
Importin subunit beta-1 OS=Mus musculus GN=Kpnb1 PE=1 SV=2	IMB1_MOUSE	97 kDa	2.4	5	12
GAS2-like protein 3 OS=Mus musculus GN=Gas2l3 PE=2 SV=1	GA2L3_MOUSE	74 kDa	2.4	5	12
LIM and SH3 domain protein 1 OS=Mus musculus GN=Lasp1 PE=1 SV=1	LASP1_MOUSE	30 kDa	2.4	5	12
Serine-threonine kinase receptor-associated protein OS=Mus musculus GN=Strap PE=1 SV=2	STRAP_MOUSE	38 kDa	2.4	5	12
DNA topoisomerase 3-beta-1 OS=Mus musculus GN=Top3b PE=2 SV=1	TOP3B_MOUSE	97 kDa	2.4	5	12
Ras GTPase-activating protein-binding protein 2 OS=Mus musculus GN=G3bp2 PE=1 SV=2	G3BP2_MOUSE	54 kDa	2.3	20	47
60S ribosomal protein L22 OS=Mus musculus GN=Rpl22 PE=2 SV=2	RL22_MOUSE	15 kDa	2.3	3	7
PR domain zinc finger protein 1 OS=Mus musculus GN=Prdm1 PE=1 SV=1	PRDM1_MOUSE	96 kDa	2.2	13	29
Eukaryotic translation initiation factor 3 subunit L OS=Mus musculus GN=Eif3l PE=1 SV=1	EIF3L_MOUSE	67 kDa	2.2	11	24
Protein Hook homolog 3 OS=Mus musculus GN=Hook3 PE=1 SV=2	HOOK3_MOUSE	83 kDa	2.2	11	24
40S ribosomal protein S15a OS=Mus musculus GN=Rps15a PE=2 SV=2	RS15A_MOUSE	15 kDa	2.2	10	22
Cytoplasmic polyadenylation element-binding protein 4 OS=Mus musculus GN=Cpeb4 PE=1 SV=1	CPEB4_MOUSE	80 kDa	2.2	8	18

Peptidyl-prolyl cis-trans isomerase A OS=Mus musculus GN=Ppia PE=1 SV=2	PPIA_MOUSE	18 kDa	2.2	6	13
Plasminogen activator inhibitor 1 RNA-binding protein OS=Mus musculus GN=Serbp1 PE=1 SV=2	PAIRB_MOUSE	45 kDa	2.2	6	13
Collagen alpha-1(I) chain OS=Mus musculus GN=Col1a1 PE=1 SV=4	CO1A1_MOUSE	138 kDa	2.2	5	11
40S ribosomal protein S24 OS=Mus musculus GN=Rps24 PE=2 SV=1	RS24_MOUSE	15 kDa	2.2	4	9
60S ribosomal protein L23 OS=Mus musculus GN=Rpl23 PE=1 SV=1	RL23_MOUSE	15 kDa	2.1	167	352
40S ribosomal protein S4, X isoform OS=Mus musculus GN=Rps4x PE=2 SV=2	RS4X_MOUSE	30 kDa	2.1	30	62
Splicing factor, proline- and glutamine-rich OS=Mus musculus GN=Sfpq PE=1 SV=1	SFPQ_MOUSE	75 kDa	2.1	18	38
60S ribosomal protein L10 OS=Mus musculus GN=Rpl10 PE=2 SV=3	RL10_MOUSE	25 kDa	2.1	18	37
Ribosome-binding protein 1 OS=Mus musculus GN=Rrbp1 PE=1 SV=2	RRBP1_MOUSE	173 kDa	2.1	15	32
Heterogeneous nuclear ribonucleoprotein M OS=Mus musculus GN=Hnrnpm PE=1 SV=3	HNRPM_MOUSE	78 kDa	2.1	14	30
ATP-dependent RNA helicase DDX1 OS=Mus musculus GN=Ddx1 PE=1 SV=1	DDX1_MOUSE	83 kDa	2.1	14	30
La-related protein 4B OS=Mus musculus GN=Larp4b PE=1 SV=2	LAR4B_MOUSE	82 kDa	2.1	13	27
40S ribosomal protein SA OS=Mus musculus GN=Rpsa PE=1 SV=4	RSSA_MOUSE	33 kDa	2.1	9	19
Heterogeneous nuclear ribonucleoprotein A1 OS=Mus musculus GN=Hnrnpa1 PE=1 SV=2	ROA1_MOUSE	34 kDa	2.1	7	15
Microtubule-associated protein 4 OS=Mus musculus GN=Map4 PE=1 SV=3	MAP4_MOUSE	117 kDa	2	64	131
Heterogeneous nuclear ribonucleoprotein K OS=Mus musculus GN=Hnrnpk PE=1 SV=1	HNRPK_MOUSE	51 kDa	2	14	28
Serine-rich coiled-coil domain-containing protein 2 OS=Mus musculus GN=Ccser2 PE=1 SV=1	CCSE2_MOUSE	93 kDa	2	11	22
Prohibitin-2 OS=Mus musculus GN=Phb2 PE=1 SV=1	PHB2_MOUSE	33 kDa	2	9	18
40S ribosomal protein S12 OS=Mus musculus GN=Rps12 PE=1 SV=2	RS12_MOUSE	15 kDa	2	8	16
KH domain-containing, RNA-binding, signal transduction-associated protein 1 OS=Mus musculus GN=Khdrbs1 PE=1 SV=2	KHDR1_MOUSE	48 kDa	2	6	12
40S ribosomal protein S23 OS=Mus musculus GN=Rps23 PE=2 SV=3	RS23_MOUSE	16 kDa	2	6	12
Transcriptional activator protein Pur-alpha OS=Mus musculus GN=Pura PE=1 SV=1	PURA_MOUSE	35 kDa	2	6	12
60S ribosomal protein L5 OS=Mus musculus GN=Rpl5 PE=1 SV=3	RL5_MOUSE	34 kDa	2	5	10
rRNA 2'-O-methyltransferase fibrillarin OS=Mus musculus GN=Fbl PE=2 SV=2	FBRL_MOUSE	34 kDa	2	5	10
Paraspeckle component 1 OS=Mus musculus GN=Pspc1 PE=1 SV=1	PSPC1_MOUSE	59 kDa	2	5	10
Titin OS=Mus musculus GN=Ttn PE=1 SV=1	TITIN_MOUSE	3906 kDa	2	4	8
60S ribosomal protein L36a OS=Mus musculus GN=Rpl36a PE=3 SV=2	RL36A_MOUSE	12 kDa	2	4	8
Uracil phosphoribosyltransferase homolog OS=Mus musculus GN=Uprt PE=2 SV=1	UPP_MOUSE	34 kDa	2	4	8

V-type proton ATPase subunit G 1 OS=Mus musculus GN=Atp6v1g1 PE=2 SV=3	VATG1_MOUSE	14 kDa	2	4	8
Myelin basic protein OS=Mus musculus GN=Mbp PE=1 SV=2	MBP_MOUSE	27 kDa	2	4	8
Growth arrest and DNA damage-inducible proteins-interacting protein 1 OS=Mus musculus GN=Gadd45gip1 PE=2 SV=1	G45IP_MOUSE	26 kDa	2	4	8
Ig mu chain C region OS=Mus musculus GN=Ighm PE=1 SV=2	IGHM_MOUSE	50 kDa	2	4	8
39S ribosomal protein L41, mitochondrial OS=Mus musculus GN=Mrpl41 PE=2 SV=1	RM41_MOUSE	15 kDa	2	4	8
Uridine-cytidine kinase-like 1 OS=Mus musculus GN=Uckl1 PE=2 SV=1	UCKL1_MOUSE	61 kDa	2	3	6
Elongation factor Tu, mitochondrial OS=Mus musculus GN=Tufm PE=1 SV=1	EFTU_MOUSE	50 kDa	2	3	6
Phenylalanine--tRNA ligase alpha subunit OS=Mus musculus GN=Farsa PE=2 SV=1	SYFA_MOUSE	58 kDa	2	3	6
AFG3-like protein 2 OS=Mus musculus GN=Afg3l2 PE=1 SV=1	AFG32_MOUSE	90 kDa	2	3	6
Eukaryotic translation initiation factor 3 subunit F OS=Mus musculus GN=Eif3f PE=1 SV=2	EIF3F_MOUSE	38 kDa	2	3	6
Spermatogenesis-associated serine-rich protein 2 OS=Mus musculus GN=Spats2 PE=1 SV=1	SPAS2_MOUSE	59 kDa	2	3	6
Peroxiredoxin-2 OS=Mus musculus GN=Prdx2 PE=1 SV=3	PRDX2_MOUSE	22 kDa	2	3	6
60S ribosomal protein L35a OS=Mus musculus GN=Rpl35a PE=2 SV=2	RL35A_MOUSE	13 kDa	2	2	4
Girdin OS=Mus musculus GN=Ccdc88a PE=1 SV=2	GRDN_MOUSE	216 kDa	2	2	4
ATP-dependent Clp protease ATP-binding subunit clpX-like, mitochondrial OS=Mus musculus GN=Clpx PE=1 SV=2	CLPX_MOUSE	69 kDa	2	2	4
Elongation factor 1-delta OS=Mus musculus GN=Eef1d PE=1 SV=3	EF1D_MOUSE	31 kDa	2	2	4
Pyruvate dehydrogenase E1 component subunit beta, mitochondrial OS=Mus musculus GN=Pdhb PE=1 SV=1	ODPB_MOUSE	39 kDa	2	2	4
RNA-binding protein PNO1 OS=Mus musculus GN=Pno1 PE=2 SV=1	PNO1_MOUSE	27 kDa	2	2	4
Stress-induced-phosphoprotein 1 OS=Mus musculus GN=Stip1 PE=1 SV=1	STIP1_MOUSE	63 kDa	2	2	4
Vacuolar protein sorting-associated protein 16 homolog OS=Mus musculus GN=Vps16 PE=1 SV=3	VPS16_MOUSE	95 kDa	2	2	4
Vesicle transport through interaction with t-SNAREs homolog 1B OS=Mus musculus GN=Vti1b PE=1 SV=1	VTI1B_MOUSE	27 kDa	2	2	4
NADH dehydrogenase [ubiquinone] 1 alpha subcomplex subunit 12 OS=Mus musculus GN=Ndufa12 PE=2 SV=2	NDUAC_MOUSE	17 kDa	2	2	4
Cysteine-rich protein 1 OS=Mus musculus GN=Crip1 PE=2 SV=2	CRIP1_MOUSE	9 kDa	2	2	4
NADH dehydrogenase [ubiquinone] 1 alpha subcomplex subunit 2 OS=Mus musculus GN=Ndufa2 PE=1 SV=3	NDUA2_MOUSE	11 kDa	2	2	4
Poly [ADP-ribose] polymerase 12 OS=Mus musculus GN=Parp12 PE=2 SV=3	PAR12_MOUSE	80 kDa	2	2	4
Terminal uridylyltransferase 7 OS=Mus musculus GN=Zcchc6 PE=2 SV=3	TUT7_MOUSE	169 kDa	2	2	4
Uridine-cytidine kinase 1 OS=Mus musculus GN=Uck1 PE=2 SV=2	UCK1_MOUSE	31 kDa	2	2	4

Ig kappa chain V-V region MOPC 21 OS=Mus musculus PE=1 SV=1	KV5A2_MOUSE	15 kDa	2	2	2
Putative pre-mRNA-splicing factor ATP-dependent RNA helicase DHX15 OS=Mus musculus GN=Dhx15 PE=2 SV=2	DHX15_MOUSE	91 kDa	2	1	2
Ribosomal protein 63, mitochondrial OS=Mus musculus GN=Mrp63 PE=2 SV=1	RT63_MOUSE	12 kDa	2	1	2
Alpha-2-macroglobulin OS=Mus musculus GN=A2m PE=1 SV=3	A2M_MOUSE	166 kDa	2	1	2
Protein FAM110B OS=Mus musculus GN=Fam110b PE=2 SV=1	F110B_MOUSE	40 kDa	2	1	2
Heat shock 70 kDa protein 4 OS=Mus musculus GN=Hspa4 PE=1 SV=1	HSP74_MOUSE	94 kDa	2	1	2
H/ACA ribonucleoprotein complex subunit 1 OS=Mus musculus GN=Gar1 PE=2 SV=1	GAR1_MOUSE	23 kDa	2	1	2
Trinucleotide repeat-containing gene 6B protein OS=Mus musculus GN=Tnrc6b PE=2 SV=2	TNR6B_MOUSE	192 kDa	2	1	2
Baculoviral IAP repeat-containing protein 6 OS=Mus musculus GN=Birc6 PE=1 SV=2	BIRC6_MOUSE	532 kDa	2	1	2
Large subunit GTPase 1 homolog OS=Mus musculus GN=Lsg1 PE=2 SV=2	LSG1_MOUSE	73 kDa	2	1	2
Heterogeneous nuclear ribonucleoprotein L-like OS=Mus musculus GN=Hnrnpll PE=1 SV=3	HNRLL_MOUSE	64 kDa	2	1	2
PAP-associated domain-containing protein 5 OS=Mus musculus GN=Papd5 PE=1 SV=2	PAPD5_MOUSE	70 kDa	2	1	2
Serine/threonine-protein phosphatase 6 regulatory subunit 1 OS=Mus musculus GN=Ppp6r1 PE=1 SV=1	PP6R1_MOUSE	95 kDa	2	1	2
28S ribosomal protein S21, mitochondrial OS=Mus musculus GN=Mrps21 PE=2 SV=1	RT21_MOUSE	11 kDa	2	1	2
Complement C1q subcomponent subunit C OS=Mus musculus GN=C1qc PE=2 SV=2	C1QC_MOUSE	26 kDa	2	1	2
GAS2-like protein 1 OS=Mus musculus GN=Gas2l1 PE=2 SV=1	GA2L1_MOUSE	72 kDa	2	1	2
Aminoacyl tRNA synthase complex-interacting multifunctional protein 2 OS=Mus musculus GN=Aimp2 PE=1 SV=2	AIMP2_MOUSE	35 kDa	2	1	2
Dolichyl-diphosphooligosaccharide--protein glycosyltransferase subunit 1 OS=Mus musculus GN=Rpn1 PE=2 SV=1	RPN1_MOUSE	69 kDa	2	1	2
39S ribosomal protein L23, mitochondrial OS=Mus musculus GN=Mrpl23 PE=2 SV=1	RM23_MOUSE	17 kDa	2	1	2
General transcription factor IIF subunit 2 OS=Mus musculus GN=Gtf2f2 PE=1 SV=1	T2FB_MOUSE	28 kDa	2	1	2
Elongation factor 1-beta OS=Mus musculus GN=Eef1b PE=1 SV=5	EF1B_MOUSE	25 kDa	2	1	2
mRNA-capping enzyme OS=Mus musculus GN=Rngtt PE=1 SV=1	MCE1_MOUSE	69 kDa	2	1	2
6-phosphofructokinase type C OS=Mus musculus GN=Pfkp PE=1 SV=1	K6PP_MOUSE	85 kDa	2	1	2
Cell division control protein 42 homolog OS=Mus musculus GN=Cdc42 PE=1 SV=2	CDC42_MOUSE	21 kDa	2	1	2
Proline-rich nuclear receptor coactivator 2 OS=Mus musculus GN=Pnrc2 PE=2 SV=1	PNRC2_MOUSE	15 kDa	2	1	2
UPF0688 protein C1orf174 homolog OS=Mus musculus PE=1 SV=1	CA174_MOUSE	25 kDa	2	1	2

G-protein-signaling modulator 3 OS=Mus musculus GN=Gpsm3 PE=1 SV=2	GPSM3_MOUSE	18 kDa	2	1	2
Heterogeneous nuclear ribonucleoprotein D0 OS=Mus musculus GN=Hnrnpd PE=1 SV=2	HNRPD_MOUSE	38 kDa	2	1	2

The blue-highlights are proteins examined by co-IPs in 293-T cells. The yellow-highlight is a PLEKHM1-binding protein recently identified by Witwicka et al (3).

Table 6. Antibodies.

Name	Sources	Catalog #	Applications	Dilutions
mouse monoclonal anti-actin	GenScript	A00702	WB	2000
rabbit polyclonal anti-ATG12	Cell Signaling	2011	WB	1000
mouse monoclonal anti-Cathepsin K	EMD Millipore	MAB3324	WB, IF	WB: 5000; IF:300
rabbit polyclonal anti-cfms	Cell Signaling	3152	WB	1000
mouse monoclonal anti-EEA1	BD Biosciences	610456	IF	300
rabbit polyclonal anti-EGF-R	EMD Millipore	06-847	WB	1000
mouse monolonal anti-FLAG (M2)	Sigma-Aldrich	F1804	WB	2000
mouse monoclonal anti-FLAG-HRP	Sigma-Aldrich	A8592	WB	2000
mouse monoclonal anti-GM130	BD Biosciences	610822	IF	250
mouse monoclonal anti-GS28	BD Biosciences	611184		250
mouse monolonal anti-HA	Covance	MMS-101P	WB	1000
rabbit monolonal anti-HA	Cell Signaling	3724	WB	2000
rat monoclonal anti-LAMP-2	Developmental Studies Hybridoma Bank	GL2A7	IF	300
rat monoclonal anti-LAMP-2	Developmental Studies Hybridoma Bank	ABL-93	WB	1000
anti-LAMP-1	Developmental Studies Hybridoma Bank	1D4B	IF	300
rabbit polyconal anti-LC3	Cell Signaling	4108	WB	1000
mouse monoclonal anti-mTOR	Cell Signaling	4517	WB	1000
rabbit polyclonal anti-phospho-mTOR (ser2448)	Cell Signaling	2971	WB	1000
mouse monoclonal anti-myc (9E10)	EMD Millipore	05-419	WB	1000
mouse monoclonal anti-myc-HRP (4A6)	EMD Millipore	16-213	WB	1000
rabbit polyconal anti-NFATc1	Santa Cruz Biotechnology	sc-7294	WB	500
rabbit polyclonal anti-TFEB	Bethyl	A303-673A	WB	2000
Goat polyclonal anti-TFEB	Thermo-Fisher	PA1-31552	IF	200
chicken polyclonal anti-human transferrin	EMD Millipore	AB3467	IF	300
mouse monoclonal anti-transferrin receptor (H68.4)	Life Technologies	13-6800	IF	300
mouse monoclonal anti-beta tubulin	Sigma-Aldrich	T5201	WB, IF	WB:5000; IF:500

Table 7. Sequences of cloning primers

Name	Sequence
HA-*Plekhm1* (Xho-I) for	5'-ATATCTCGAGGAAATGTATCCTTACGATGTGCCTGATTATGCACTCT CAGTGGAGAATGGCCTG-3'
Plekhm1 (Not-I) rev	5'-ATATATATTGCGGCCGCTTAACTGACAACGTTCTGTTCCTG-3'
Plekhm1-hu (Not-I) rev	5'-ATATATATGCGGCCGCTCATCTGTGGGTGATGGCTTTCAG-3'
Plekhm1-ia (Not-I) rev	5'-ATATATATGCGGCCGCCTAGGCTGTGGAGGGAGAGGGCGTCTGGA ACATGGGGGTGTC-3'
Plekhm1-R714C-for	5'-CTGTATGCAGACTGTACCTGGGTCCCCTATATCTTTTCCCTG-3'
Plekhm1-R714C-rev	5'-GGACCCAGGTACAGTCTGCATACAGATACAAAAGGGAC-3'
Plekhm1-ΔRUN (Xho-I) for	5'-TATCTCGAGATGTATCCTTACGATGTGCCTGATTATGCAATCTTAAAT GAATGGACACTC-3'
Plekhm1-ΔPH1 for	5'-CCATTCCGGGGCCGCCCTCAGCAGGAAGATGAG-3'
Plekhm1-ΔPH1 rev	5'-CTGCTGAGGGCGGCCCCGGAATGGGTTGGACAG-3'
Plekhm1-ΔPH2 for	5'-GAACCAGATGCTCTAGAGTCAGCTGAGGAGGCTG-3'
Plekhm1-ΔPH2 rev	5'-GCTGACTCTAGAGCATCTGGTTCTGGAACCTG-3'
Plekhm1-ΔPH for	5'-CCATTCCGGGGCCTAGAGTCAGCTGAGGAGGCTG-3'
Plekhm1-ΔPH rev	5'-CTGACTCTAGGCCCCGGAATGGGTTGGACAG-3'
Plekhm1-ΔC1 (Not-I) rev	5'-ATATATATGCGGCCGCTTACTGGGATGCGAATTCAATCAG-3'
Plekhm1-N (Not-I) rev	5'-ATATATATGCGGCCGCTTATTGCCTTCGGTGCACCACACAG-3'
HA-*Plekhm1*-C (Xho-I) for	5'-ATATCTCGAGATGTATCCTTACGATGTGCCTGATTATGCAGTGCCCT CACAGGCCTGTG-3'
Plekhm1$^{Y949A/L950A}$ for	5'-ACTTCTGGGGGACGCCGCGGGCCTGTGCCGAAGTGGTGC-3'
Plekhm1$^{Y949A/L950A}$ rev	5'-TTCGGCACAGGCCCGCGGCGTCCCCCAGAAGTTTCAGCTGC-3'
Def8 (BamH-I) for	5'- ATTGGATCCGCTATGGAATATGATGAGAAGCTG-3'
Def8-FLAG (Xho-I) rev	5'-ATCGCTCGAGCTACTTGTCGTCATCGTCTTTGTAGTCGGCATCCATG TCTAGGCCAGG-3'
Myc-*Def8* (BamH-I) for	5'-ATTGGATCCGCCGCCATGGAGCAGAAACTCATCTCTGAAGAGGATC TGAATGAAGAATATGATGAGAAGCTGGTTC-3'
Def8 (Xho-I) rev	5'-ATCGCTCGAGCTAGGCATCCATGTCTAGGCCAGG-3'
Kifc1 (Xho-I) for	5'-ATCGCTCGAGACCATGGACGTGCAGGCGCAG-3'
Kifc1-FLAG (Sac-II) rev	5'-AATTCCGCGGTCACTTGTCGTCATCGTCTTTGTAGTCCTTCTTATT AGCCTGAGCAGTAC-3'
Clasp2 (BamH-I) for	5'-ATTGGATCCGGAATGAGGCGGCTGATTTGC-3'

Clasp2-FLAG (Xho-I) rev	5'-ATCGCTCGAGCTACTTGTCGTCATCGTCTTTGTAGTCACTCTGTCCAGAAACATCAGC-3'
Tpx2 (Xho-I) for	5'-ATCGCTCGAGGGCAATGTCACAAGTCCCTAC-3'
Tpx2-FLAG (Sac-II) rev	5'-ATATCCGCGGCTACTTGTCGTCATCGTCTTTGTAGTCCTGGAACCGAGTGGAGAAC-3'
Fam98a (BamH-I) for	5'-ATTGGATCCGCCGCCATGGAGACTGACATCTTGGAG-3'
Fam98a-FLAG (EcoR-I) rev	5'-ATTGAATTCTCACTTGTCGTCATCGTCTTTGTAGTCACTAGTATAATGTCTTCCTTGTC-3'
Ndel1 (BamH-I) for	5'-ATTGGATCCTGATCATGGATGGTGAAGATATAC-3'
Ndel1-FLAG (Xho-I) rev	5'-ATCGCTCGAGTCACTTGTCGTCATCGTCTTTGTAGTCCACACTGAGAGGCAGCATAC-3'
Map3k7 (BamH-I) for	5'-ATTGGATCCGATCATGTCGACAGCCTCCG-3'
Map3k7-FLAG (Xho-I) rev	5'-ATCGCTCGAGTCACTTGTCGTCATCGTCTTTGTAGTCTGAAGTGCCTTGTCGTTTCTG-3'
Rap1b (BamH-I) for	5'-ATTGGATCCACCATGCGTGAATATAAGCTCG-3'
Rap1b-FLAG (Xho-I) rev	5'-ATCGCTCGAGTTACTTGTCGTCATCGTCTTTGTAGTCAAGCAGCTGACACGATGACTTT-3'
Lamp-2a (EcoR-I) for	5'-ATCGGAATTCACGATGTGCCTCTCTCCG -3'
Lamp-2a (BamH-I) rev	5'-AATTGGATCCCGTCCTCCACCGCCTCCAAATTGCTCATATCCAGTATG -3'
eGfp (Xho-I) rev	5'- ATATCTCGAGTTACTTGTACAGCTCGTCCATGC-3'
FLAG-*Rab7* (Xho-I) for	5'-ATATCTCGAGATGGACTACAAAGACGATGACGACAAGACCTCTAGGAAGAAAGTGTTG-3'
Rab7 (Not-I) rev	5'-ATATATATGCGGCCGCTCAACAACTGCAGCTTTCTGC-3'

References

1. Takeshita, S., Kaji, K., and Kudo, A. 2000. Identification and characterization of the new osteoclast progenitor with macrophage phenotypes being able to differentiate into mature osteoclasts. *J Bone Miner Res* 15:1477-1488.
2. Xu, J. 2005. Preparation, culture, and immortalization of mouse embryonic fibroblasts. *Curr Protoc Mol Biol* Chapter 28:Unit 28 21.
3. Witwicka, H., Jia, H., Kutikov, A., Reyes-Gutierrez, P., Li, X., and Odgren, P.R. 2015. TRAFD1 (FLN29) Interacts with Plekhm1 and Regulates Osteoclast Acidification and Resorption. *PLoS One* 10:e0127537.

Full unedited blot images for Figure 4 & 6

Figure 4C

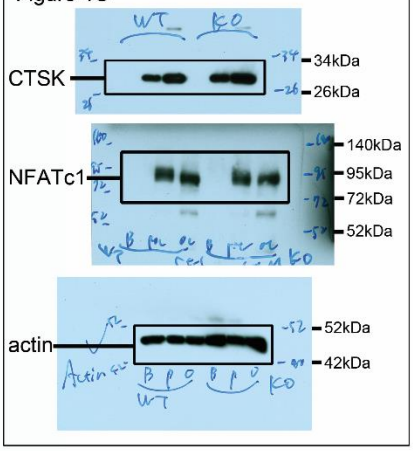

Figure 6B

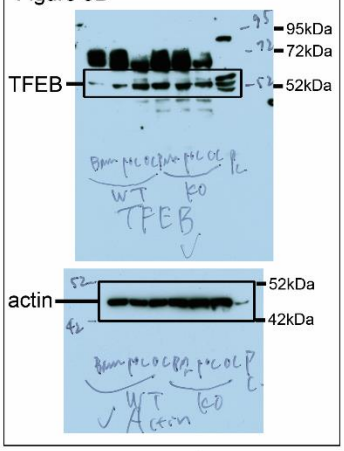

Figure 6C

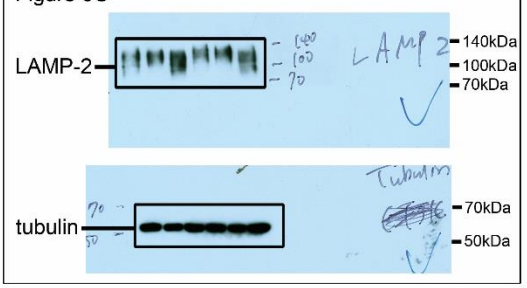

Figure 6D

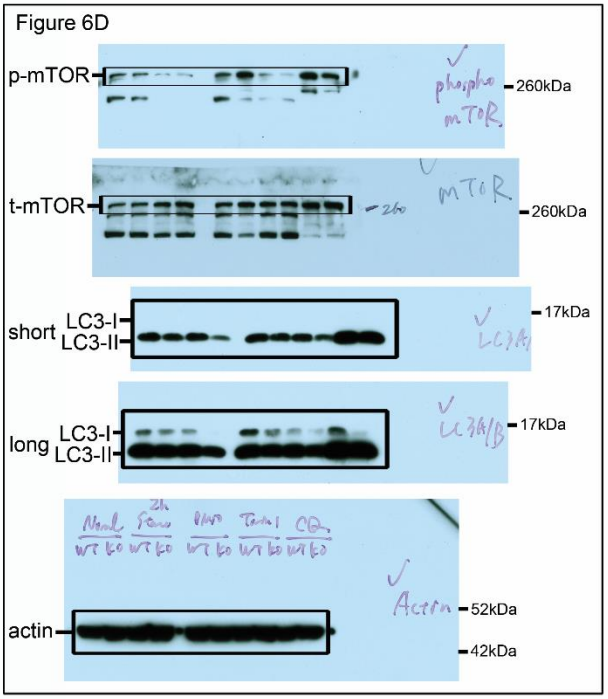

Figure 6E

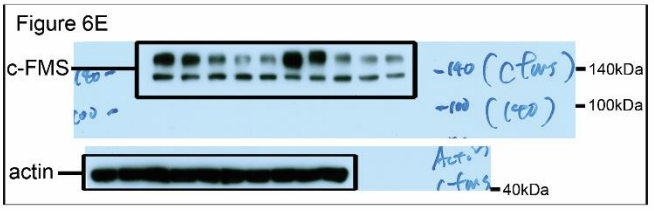

Figure 6F

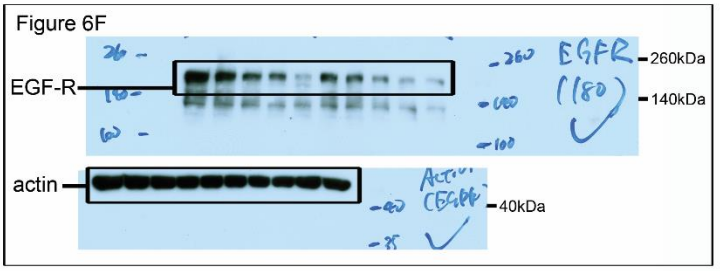

Full unedited blot images for Figure 7

Figure 7A

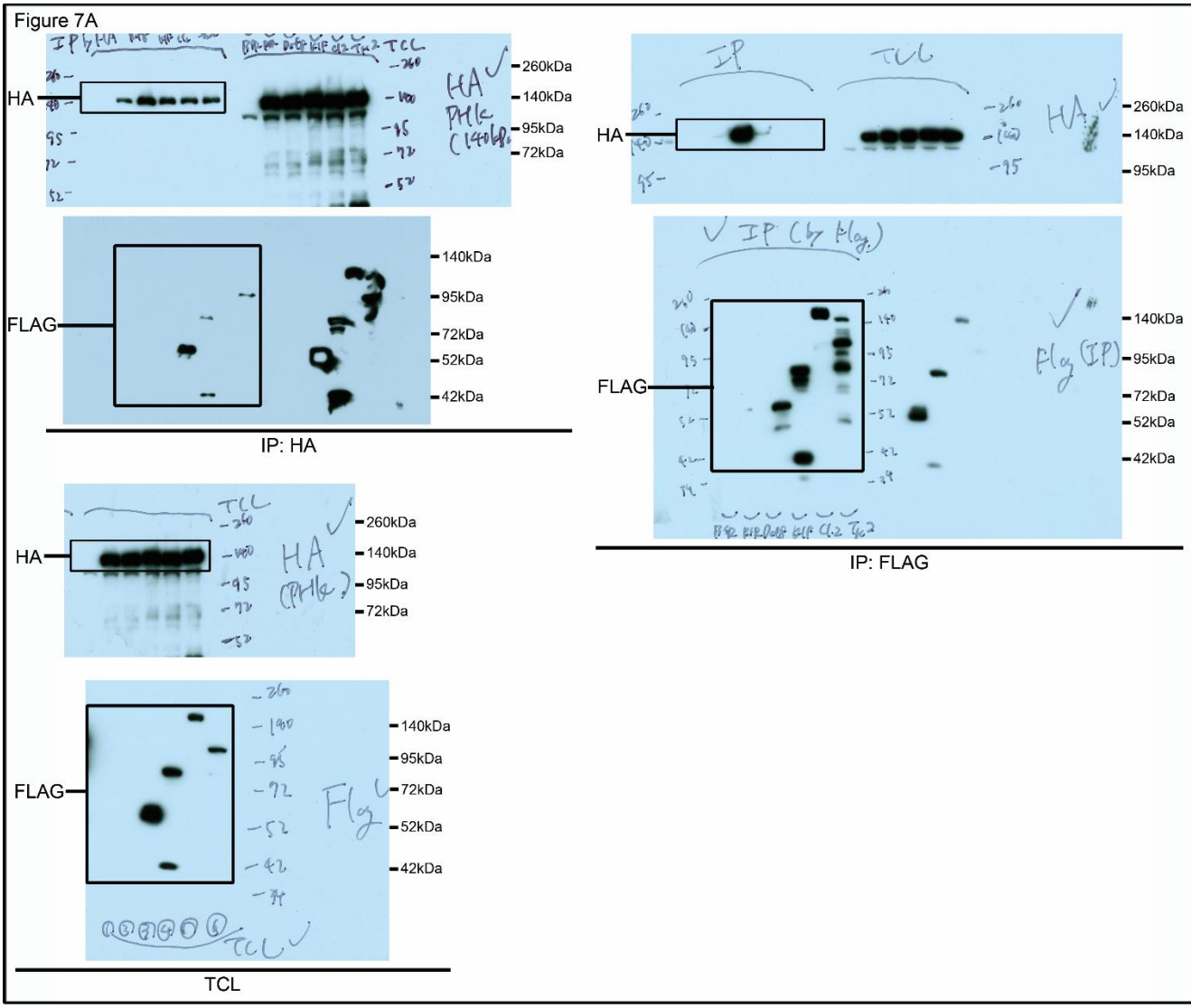

Full unedited blot images for Figure 7 & 9

Figure 7C

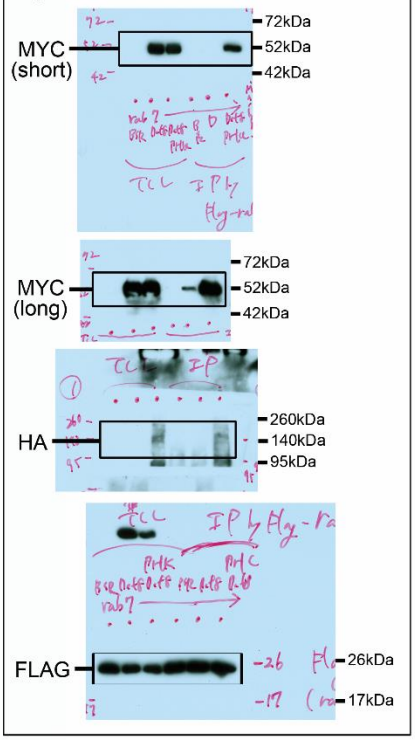

Figure 7D

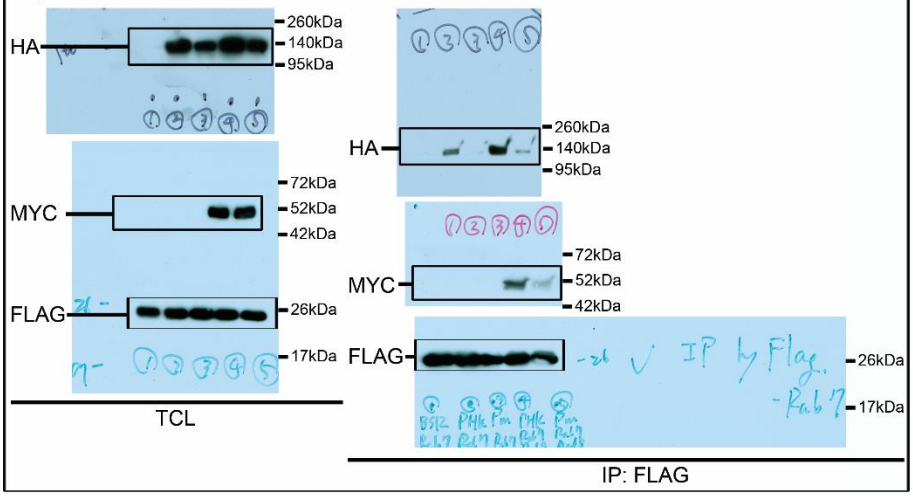

Figure 9A

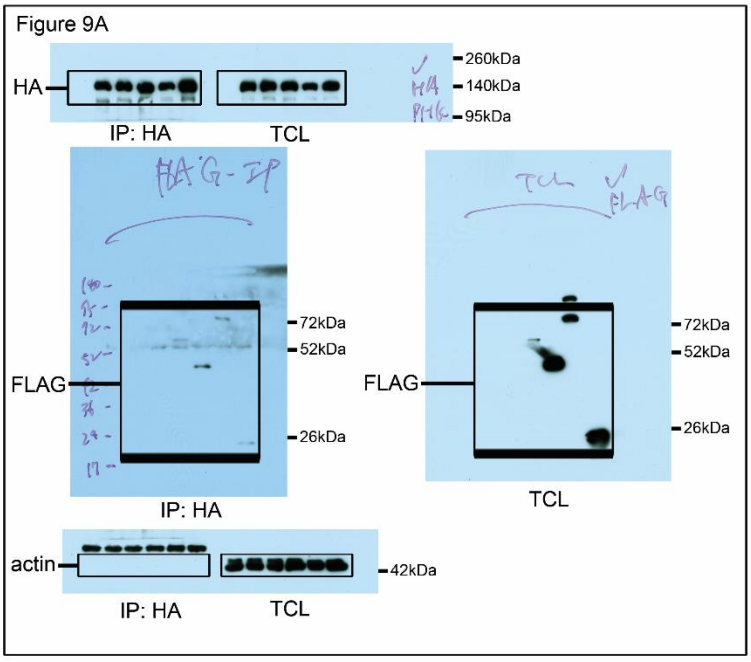

Full unedited blot images for Figure 9

Figure 9B

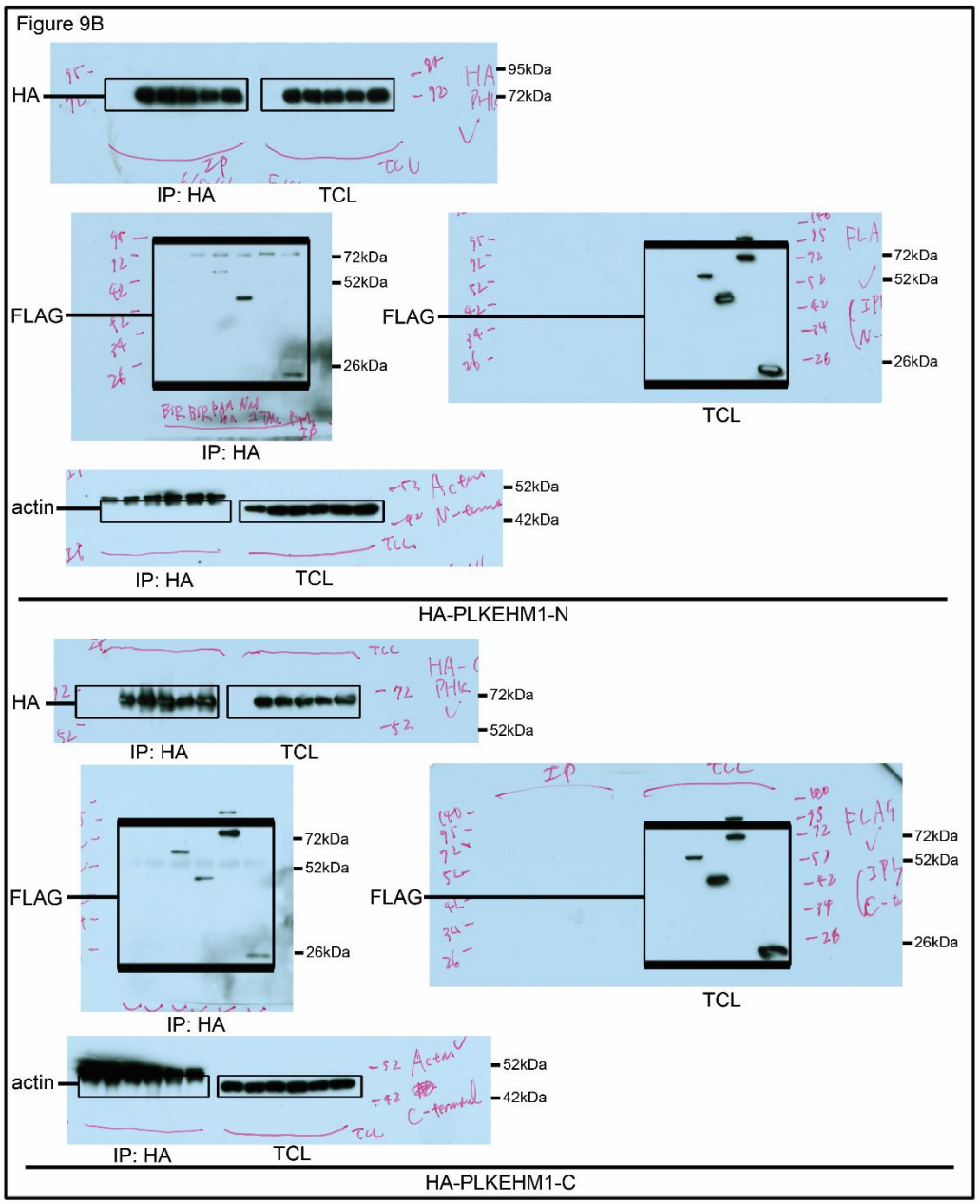

Full unedited blot images for Supplemental Figure 4, 5, 13, & 14

Supplemental Figure 4C

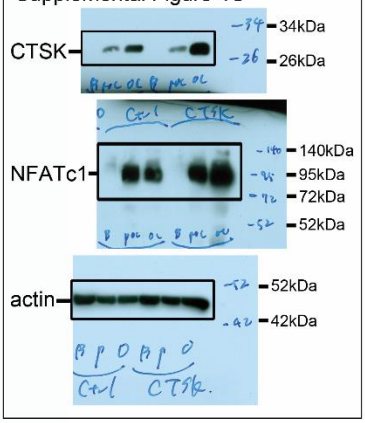

Supplemental Figure 5

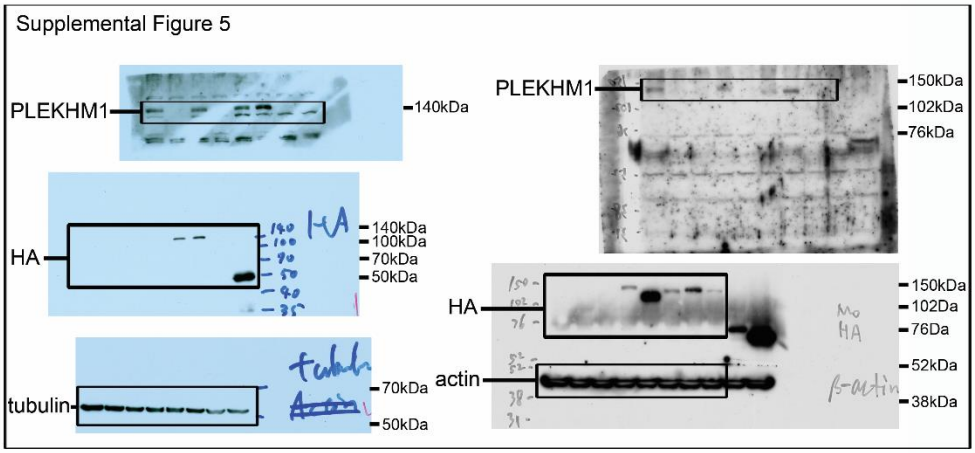

Supplemental Figure 13A

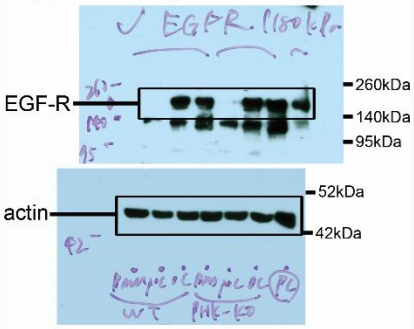

Supplemental Figure 14A

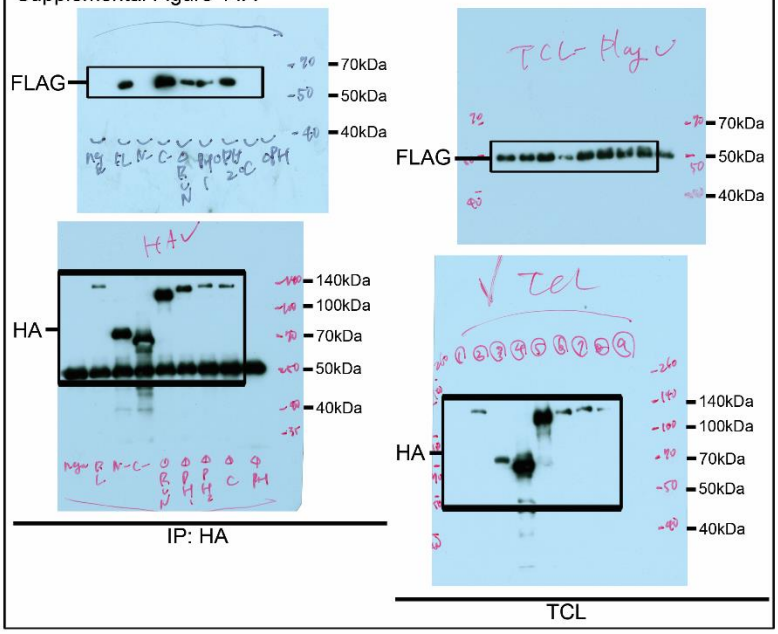

Full unedited blot images for Supplemental Figure 14 & 15

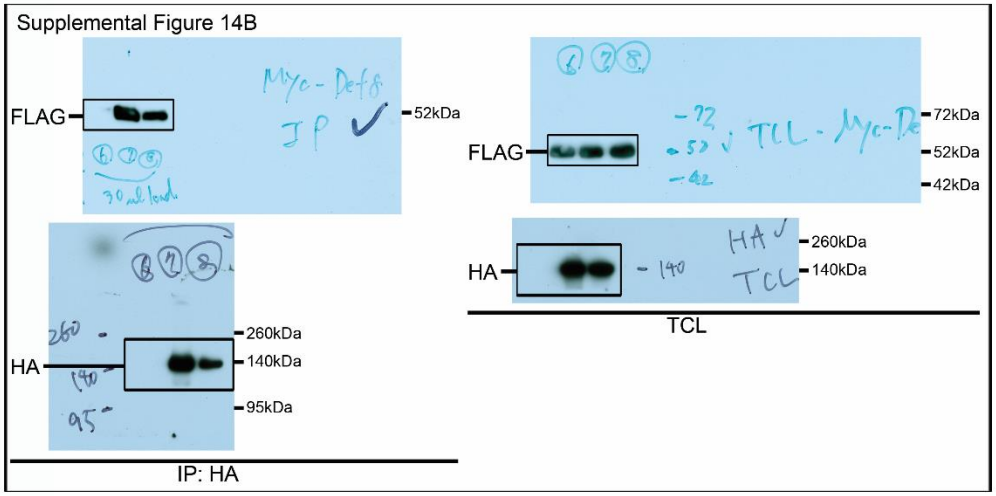

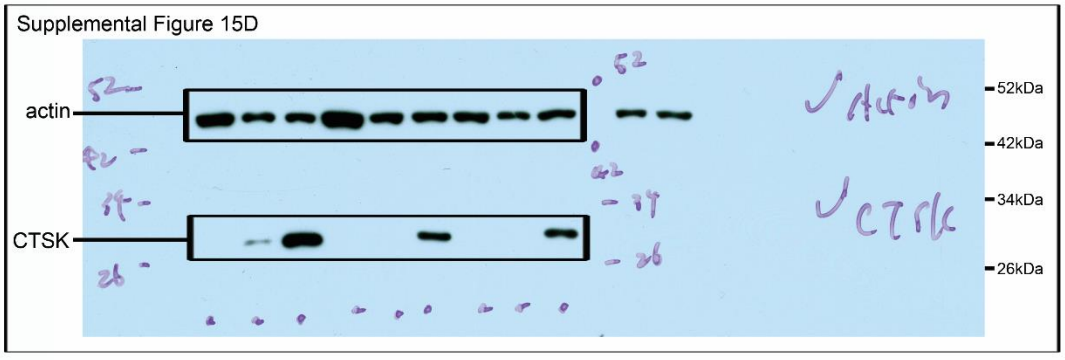

Full unedited blot images for Supplemental Figure 16

Supplemental Figure 16A FAM98A

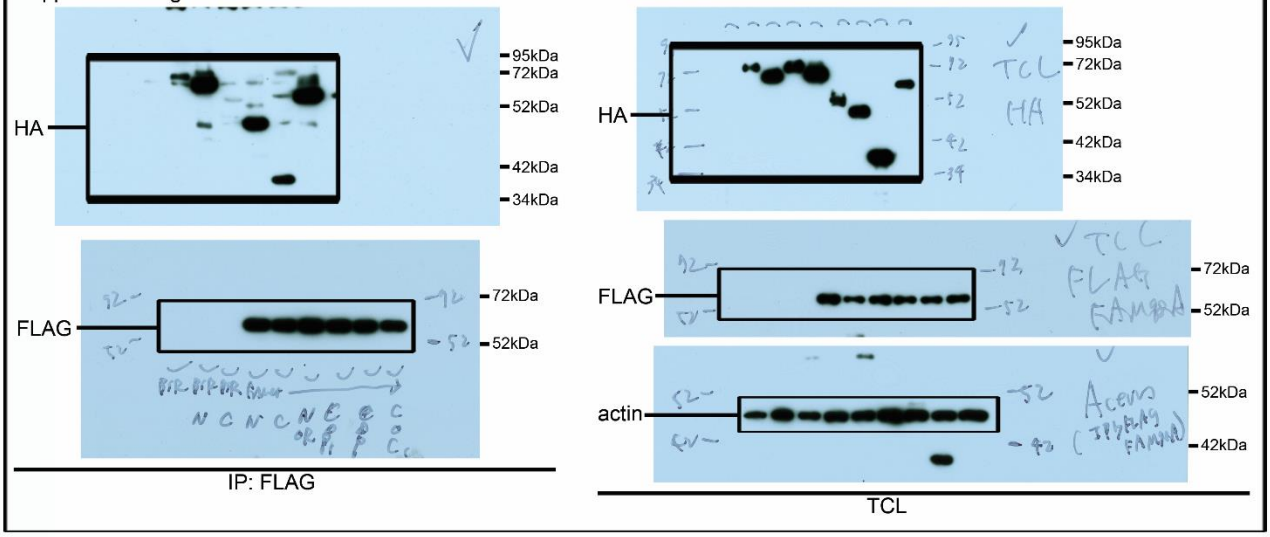

Supplemental Figure 16B NDEL1